

Climatic patterns revealed by pollen and oxygen isotope records across the Matuyama–Brunhes Boundary in the central Mediterranean (southern Italy)

L. CAPRARO¹, A. ASIOLI², J. BACKMAN³, R. BERTOLDI⁴, J.E.T. CHANNELL⁵,
F. MASSARI⁶ & D. RIO⁶

¹*Dipartimento di Geologia, Paleontologia e Geofisica, Università di Padova, Via Giotto
1 I-35137 Padova, Italy (e-mail: luca.capraro@unipd.it)*

²*Istituto di Geoscienze e Georisorse C.N.R., c/o Dipartimento di Mineralogia e Petrologia,
Università di Padova, Corso Garibaldi 37 I-35137 Padova, Italy*

³*Department of Geology and Geochemistry, Stockholm University, S-106 91 Stockholm, Sweden*

⁴*Dipartimento di Biologia Evolutiva e Funzionale, Università di Parma, Viale delle Scienze
I-43100 Parma, Italy*

⁵*Department of Geological Sciences, POB 112120, University of Florida, Gainesville,
FL 32611, USA*

⁶*Dipartimento di Geologia, Paleontologia e Geofisica, Università di Padova, Via Giotto
1 I-35137 Padova, Italy*

Abstract: A c. 50 m thick section located in the Crotone Basin (southern Italy) was investigated using oxygen isotopes, pollen and planktonic foraminifera. The section records two complete transgressive–regressive cycles mainly driven by glacio-eustasy. Biostratigraphy and oxygen isotope chronology indicate that the section spans from Marine Isotope Stage (MIS) 22 (c. 0.87 Ma) to MIS 18.3 (c. 0.73 Ma), thus straddling the Matuyama–Brunhes (M–B) boundary which occurs in the middle of MIS 19. The rich pollen assemblages provide a unique record of the vegetation in the central Mediterranean during the Early–Middle Pleistocene climatic transition. Interglacials are characterized by a mesothermic vegetation similar to the present day, whereas a rain-demanding conifer forest dominates the glacials of MIS 20 and MIS 18. This is unexpected because it is generally considered that during the Pleistocene, glacials in central Mediterranean were characterized by steppe (arid) conditions. By contrast, arid conditions occur during the deglaciations. These results are inconsistent with the widespread practice of linking glacials with arid conditions in the central Mediterranean during Pliocene and Early Pleistocene times. This study emphasizes the need to establish more accurate land–sea correlation.

The climatic system underwent major changes in the interval from c. 1.2 Ma (Early Pleistocene) to c. 0.6 Ma (Middle Pleistocene), known as the ‘Middle Pleistocene climatic transition’ (MPT; Raymo *et al.* 1997; Mudelsee & Schulz 1997) or the ‘mid-Pleistocene climatic revolution’ (Berger *et al.* 1994). During the Early–Middle Pleistocene climatic transition (EMPT), large ice sheets in the northern hemisphere became established (Prell 1982; Ruddiman *et al.* 1989) and the transition occurred from a dominant 40 ka climatic cyclicity to the 100 ka glacial–interglacial cycles that have characterized the most recent part of Earth history. These changes have been the focus of intensive study in deep-sea sediments, providing information on the evolution of marine climate. Data on continental climate evolution remain sparse in spite of recent efforts on lacustrine (Williams *et al.* 2001; Prokopenko *et al.*

2002) and loess (Kukla & Cilek 1996) successions. More information on continental climate evolution and its link to marine records is clearly needed, particularly to gain a better understanding of the MPT.

Pollen in continental and marine sediments represents a readily available and well-known proxy for continental climate. Pollen grains are, however, often poorly represented in deep-sea sediments, and continental records are often discontinuous and lack reliable chronological control. The shelf–upper slope depositional environment, where the record of both marine and continental climate is commonly preserved, represents a geological setting that combines the merits of deep-sea (good chronology) and continental (rich pollen content) sediments. Furthermore, sedimentary successions from the shelf–upper slope setting permit studies of the complex interplay between eustasy, tectonics and

climate, and resulting facies expressions. Coring of such sections is currently being planned by the IMAGES program (<http://www.images-pages.org/start.html>) and the Integrated Ocean Drilling Program (<http://www.iodp.org>). Shelf–upper slope sediments crop out widely on land in countries such as Japan, USA (California), New Zealand and Italy. Many of these sections are far from being fully exploited. Here we report on an interdisciplinary study of the late Neogene–Pleistocene Crotona Basin in Calabria (southern Italy, Fig. 1). The major objective is to stack a Pleistocene record of outer shelf–upper slope sediments by splicing sections from various parts of the basin to reconstruct the pattern of change in the vegetation, and hence continental climate, in a chronological framework that is directly correlated to marine climatic evolution. Knowledge of vegetation evolution and vegetation gradients across Europe in the Early and Middle Pleistocene is still not well enough documented because of limited availability of suitable sedimentary sections with continuous high sediment accumulation rates, rich fossil assemblages, and good chronological control.

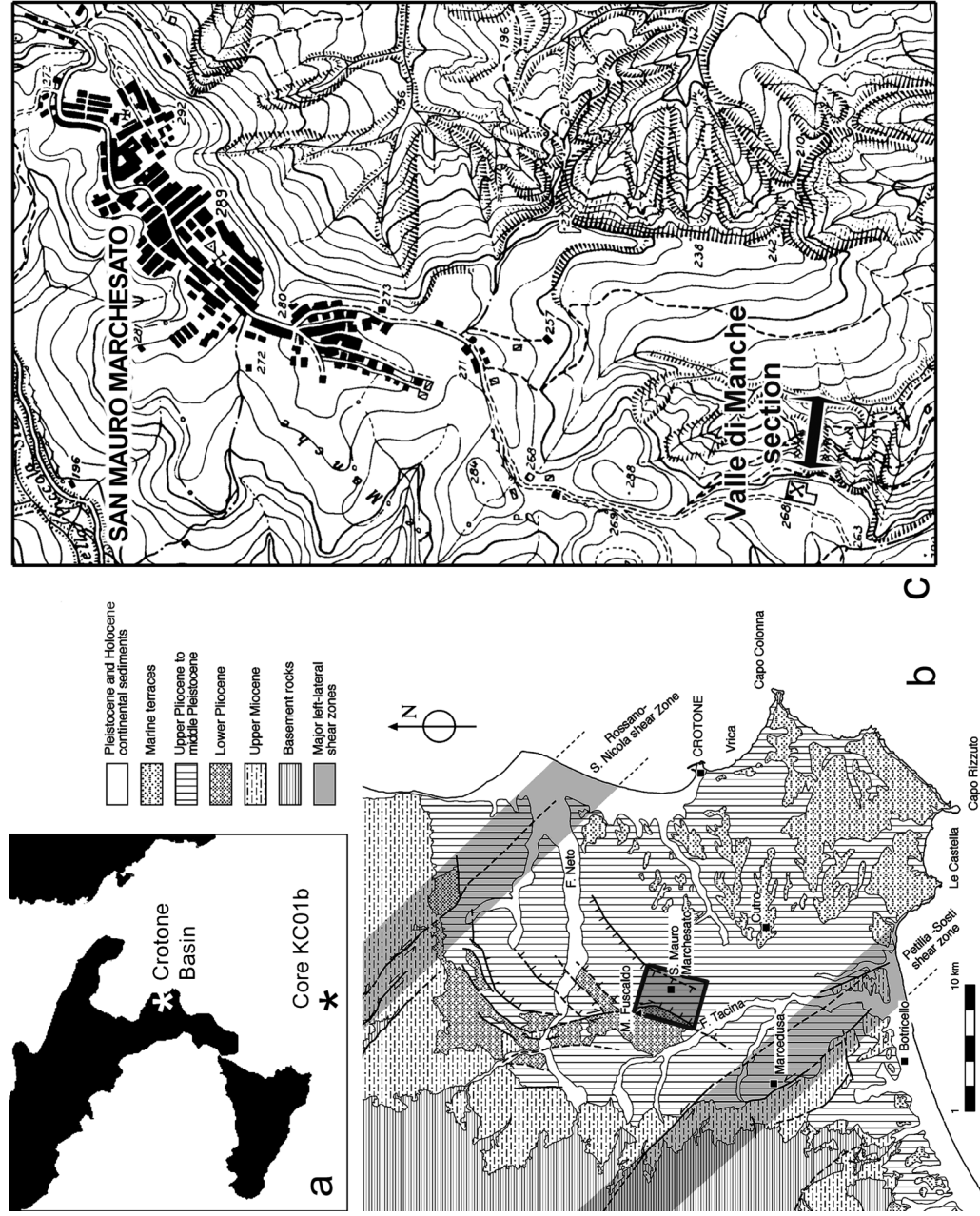
We report on results from the 200+ m thick San Mauro succession cropping out near the village of San Mauro Marchesato (Figs 1 & 2) that has been previously studied by Rio *et al.* (1996) and Massari *et al.* (2002). The lower part of the San Mauro succession was deposited in an outer shelf environment, allowing marine stratigraphic tools to be employed, but located close enough to the continent for pollen to be common to abundant. The part of the San Mauro succession considered here belongs to the Valle di Manche section and is organized into transgressive–regressive cycles (cyclothem) covering the time interval from 0.87 Ma to 0.73 Ma. The Matuyama–Brunhes boundary (M–B boundary; Fig. 2) has been recognized in the section (Rio *et al.* 1996). This geomagnetic reversal boundary, which provides a firm chronological control point, has been proposed as a suitable criterion for defining the Early–Middle Pleistocene boundary (e.g. Richmond 1996; Pillans 2003). Our study offers a glimpse into the vegetative landscape of a central Mediterranean region that is suitable for obtaining clues about the interplay between eustasy, tectonics and climate in the shaping of stratigraphic architecture of sedimentary cycles. Key objectives include: (1) to document vegetational history in the central Mediterranean; (2) to link marine and continental climates in the region by comparing oxygen isotopes, planktonic foraminifera and pollen records; and (3) to verify whether glacio–eustasy has been the main driving mechanism for the deposition of cyclothem in the San Mauro succession, as suggested by Rio *et al.* (1996) on the basis of physical stratigraphy and chronology.

Present-day environmental setting

The Crotona Basin is located at about 39°00'N and 17°04'E. The area lies in the Mediterranean evergreen biome, characterized by short, cool, rainy winters and long, warm, dry summers. The mean annual temperature in the Crotona area is about 15.6°C and the mean annual precipitation is about 630 mm/year (Frosini 1961). A strong seasonality in climate is present because of the dramatic gap between the summer minimum rainfall (June, 9 mm/month) and winter maximum (December, 110 mm/month). Such a climate favours the development of distinct vegetation belts (Fig. 3). In the Crotona Basin, and in general in southern Italy where mountains higher than 2000 m are present, the vegetation belts are organized as follows (Noirfalise *et al.* 1987).

- (a) Thermomediterranean Belt ('Arid Mediterranean Belt' according to Pignatti 1979), composed of prostrate shrubs, maquis, matorral and steppe-like elements (e.g. *Ephedra* and *Artemisia*) that thrive along the coast, where soil conditions are poor and rainfall rates are very low. The minimum precipitation rate is in excess of 300 mm per year, since at lower values a subdesert vegetation develops (Walter 1974).
- (b) Mesomediterranean Belt ('Mediterranean Belt' according to Pignatti 1979), characterized by shrubby maquis transforming into an evergreen forest mainly dominated by *Quercus ilex* and secondarily by other evergreen oaks as well as *Pistacia*, *Olea* and *Phyllirea*. This belt is widely distributed in southern Italy up to about 1000 m above sea level. The assemblage indicates an overall dry climate (total rainfall between 450 and 600 mm per year and major seasonal contrast) with warm summers and mild winters (Suc *et al.* 1992).
- (c) Supramediterranean Belt ('Sannitic Belt' according to Pignatti 1979), characterized by mixed deciduous forest. Deciduous oaks (*Quercus*), elm (*Ulmus*), hornbeam (*Carpinus*), chestnut (*Castanea*) and others dominate this belt. Mixed oak (mesothermic) forest flourishes under a mild, seasonally driven climate with a minimum rainfall of 600 mm per year and a mean annual temperature in excess of 10°C (Fenaroli 1970). However, in the Mediterranean realm, the boundary between Mediterranean and Sannitic belts is often transitional and in some cases both belts are intermingled in a 'mixed' assemblage. The distribution of deciduous oak forests in southern Italy is nowadays limited to hilly and low mountain areas (from c. 1000 to 1500 m above sea level) and mostly

Fig. 1. Location of the study area. (a) Location of the Crotona Basin and of Core KC01b (36°15'N, 17°44'E). (b) Geological and tectonic sketch-map of the Crotona Basin (after Massari *et al.* 2002) and location of the San Mauro Marchesato area. (c) Location of the Valle di Manche section, south of the San Mauro Marchesato village (Rio *et al.* 1996; Massari *et al.* 2002).



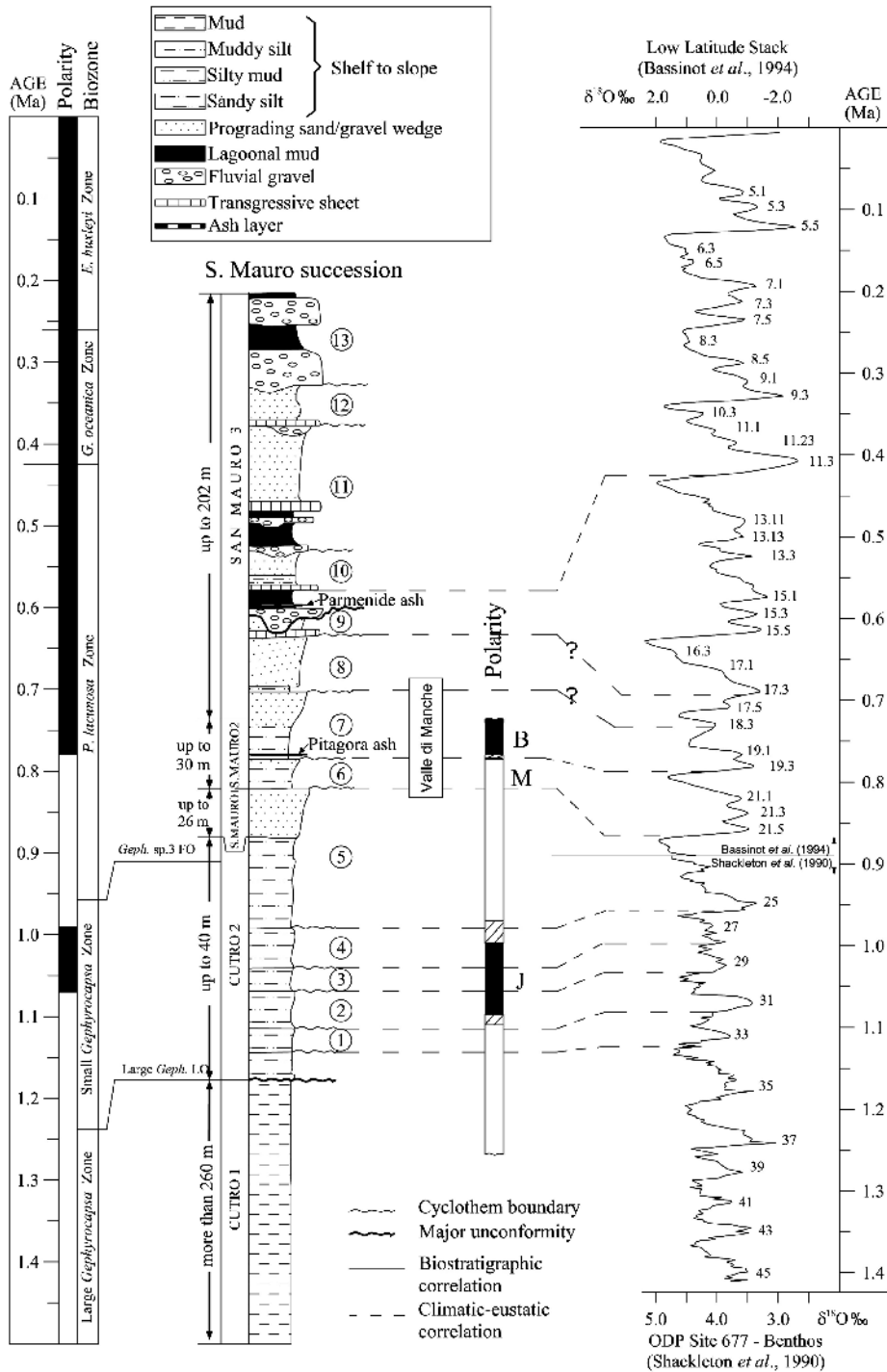


Fig. 2. The composite San Mauro succession (modified after Massari *et al.* 2002). Correlation with the standard time scale (left) is based on biomagnetostratigraphic constraints (Rio *et al.* 1996). Correlation to the standard marine isotope stratigraphy (MIS: right) is based on transgressive–regressive cycles (cyclothems) evidenced by Rio *et al.* (1996), Massari *et al.* (2002) and data reported in this paper.

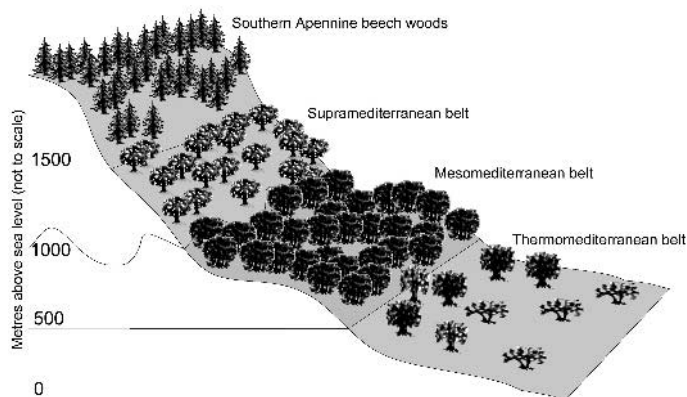


Fig. 3. Idealized sketch of the present-day composition of vegetation along the slopes of major massifs in southern Italy (after Fenaroli 1970; Pignatti 1979; Noirfalise *et al.* 1987).

controlled by water availability during the winter.

- (d) Southern Apennine Beech Woods ('Subatlantic Mountain Belt' according to Pignatti 1979), a 'cold' forest community that requires high precipitation rates and a weak seasonal contrast. In the Calabrian region, this assemblage is distributed above *c.* 1500 m above sea level, where the annual average temperature is below 10°C and precipitation is in excess of 1700 mm/year (Fenaroli 1970). Beech (*Fagus sylvatica*) is dominant on the arid eastern flanks of the Sila and Aspromonte massifs, whereas the more rainy western flanks are blanketed by large populations of the rain-demanding species *Abies alba* (silver fir). Notwithstanding their wide distribution in northern Europe and the Alps, *Picea excelsa* (Norway spruce) and *Larix europaea* (larch) are nowadays totally absent from the Calabrian massifs.

The San Mauro succession

The Lower and Middle Pleistocene San Mauro succession (Fig. 2) represents the younger part of the infilling of the late Neogene to Quaternary Crotona Basin, a forearc basin located above the internal part of the Calabrian accretionary wedge (Van Dijk 1991; Fig. 1). It crops out in the surroundings of the village of San Mauro Marchesato, in the recently uplifted Crotona peninsula (southern Italy; Fig. 1). It is confined within a small basin (the San Mauro sub-basin) bordered by two N- to NNE-trending dextral oblique-slip faults, the stratigraphic and tectonic setting of which has been the focus of a detailed integrated study by Rio *et al.* (1996) and Massari *et al.*

(1999, 2002). Facies associations and thicknesses change rapidly over short distances, due to active synsedimentary faulting and folding.

The San Mauro succession (Fig. 2) displays an overall regressive trend from slope mudstones ('Cutro Marly Clay' in Roda 1964) to a series of shallow-water to continental cyclothem (the San Mauro Sandstone; 'Molassa di San Mauro' in Roda 1964). The Cutro Marly Clay is split by a major angular unconformity into a lower unit of massive slope mudstones (Cutro 1) and an upper unit (Cutro 2) consisting of four outer- to inner-shelf cyclothem (Fig. 2). A sharp facies change marks the transition from Cutro 2 mudstones to the San Mauro Sandstone. This sandstone shows a marked cyclothem organization and has been subdivided into three subunits (Fig. 2) on the basis of the widespread, mainly pelitic, San Mauro 2 subunit. The lower cyclothem (5 to 9) were laid down in an outer shelf to near-shore environment. Transgressive events are marked by ravinement surfaces in the proximal area of the sub-basin, and generally marine flooding surfaces show down-dipping trends. The cyclothem of the upper part of the San Mauro Sandstone (cyclothem 10 to 13) are characterized by an abrupt change to a more proximal facies, with increasing amounts of marginal-marine to continental deposits. Two widely traceable volcanoclastic strata, named the Pitagora Ash and the Parmenide Ash, occur in cyclothem 7 and 10 respectively (Fig. 2), and are important key beds for regional stratigraphy.

Together, the Cutro 2 and San Mauro Sandstone consist of a stack of 13 cyclothem (Fig. 2). Available biomagnetostratigraphic constraints are highly resolved (Rio *et al.* 1996; Fig. 2) and indicate that the maximum flooding intervals of cyclothem 1 to 5 can be correlated with Marine Isotope Stage

(MIS) 33 to MIS 25. The sharp facies change at the base of the San Mauro Sandstone (within cyclothem 5), that is rich in the cold water mollusc *Arctica islandica*, correlates with the pronounced and long-lasting glacial associated with MIS 24–22. Hence, the major facies change associated with this unit may represent a sedimentary response to the apparently abrupt increase in ice volume associated with MIS 24–22 (Mudelsee & Schulz 1997). The M–B boundary, within the muddy condensed section of cyclothem 7, is nearly coincident with the Pitagora ash (Rio *et al.* 1996) and allows the correlation of the maximum flooding intervals of cyclothem 6 and 7 with MIS 21 and MIS 19, respectively. The stratigraphic record above cyclothem 7 lacks chronological constraints. However, the Parmenide ash, which is within transgressive (lagoonal) sediments of cyclothem 10 (Fig. 2), has been traced into a deeper part of the Crotone Basin (Marcedusa area), where biostratigraphy indicates a position at the transition from MIS 12 to MIS 11 (Massari *et al.* 2002).

The Valle di Manche section

Test samples were collected to investigate pollen contents in the lower part of the San Mauro succession. Cyclothem 1 to 5 yielded poor results and are not considered further here. In contrast, cyclothem 6 and 7 in the Valle di Manche section, located in a basinward subsiding area along the axes of growth synclines, yielded fairly rich pollen assemblages. This section is one of the component segments utilized by Rio *et al.* (1996) and Massari *et al.* (2002) for reconstructing the San Mauro succession and has been studied for magnetostratigraphy and calcareous nannofossil biostratigraphy (Rio *et al.* 1996). The entire section includes cyclothem 5, 6, 7 and 8 (Massari *et al.* 2002). However, in this work, we focus on the upper part of the section. We have studied cyclothem 6 and 7, and isolated samples from cyclothem 5 and 8 (Fig. 4). The sampled interval is 50 m thick. Due to the basinal setting, surfaces indicative of various system tracts of depositional sequences are subtle or absent. However, the cyclothem nature of the section is represented by the rhythmic repetition of facies as reported in Figure 4 and Table 1. Particularly evident are the two muddy intervals (Facies A) that, also on the basis of faunal evidence, can be interpreted as maximum-flooding condensed intervals. In both cyclothem, the muddy intervals of Facies A are followed by intervals (Facies B1) punctuated by repeated development of firm grounds that are mantled by clumps of *Neopycnodonte cochlear*. Outer-shelf palaeodepths, in the order of 100–150 m, are indicated in the condensed section. The dominant *Uvigerina peregrina*–*Brizalina*–*Bulimina marginata* assemblage

suggests fine-grained substrates, high fluxes of organic matter and/or low levels of oxygenation in the interstitial waters. An upward-shallowing trend begins from the top of the *Neopycnodonte*-bearing interval in both cyclothem (6 and 7). However, the ‘regressive’ portion differs in the two cyclothem, showing much coarser-grained facies in cyclothem 7 (Fig. 4 & Table 1).

Material and methods

The stratigraphic positions of samples collected for analysis are given in Figure 4. Planktonic foraminifera are present only up to the 63 m level in the section, whereas pollen are common to abundant throughout. Considering an average accumulation rate of 35 cm/ka, based on the chronology developed by Rio *et al.* (1996), a sampling resolution of about 2900 years is attained. However, we will show that sediment accumulation rates are highly variable along the section and sampling resolution is quite different in the relatively condensed cyclothem 6 in comparison to the expanded cyclothem 7.

Isotopes

Oxygen isotope stratigraphy has been established for the benthic foraminifera *Uvigerina peregrina* and for the planktonic foraminifera *Globigerinoides ruber* and *Globorotalia inflata* in 51 samples from the topmost cyclothem 5, the entire cyclothem 6 and the lowermost cyclothem 7. Hand-picked specimens showing no traces of diagenetic alteration were selected under an optical stereomicroscope. Foraminiferal samples were ultrasonically cleaned in order to remove contaminants (coccoliths, overgrowths, and detrital infilling) and roasted under vacuum at about 350°C for two hours. Analyses were carried out on a Finnigan MAT 252 mass spectrometer. The results are expressed as per mil (‰) deviation with respect to the international Peedee belemnite (PDB) standard. The reproducibility of the measurements is $\pm 0.1\%$. The stable oxygen isotope data are presented in Table 2 and Figure 5.

Planktonic foraminifera

For planktonic and benthic foraminifera the samples were weighed, washed with a mesh width of 61 μm , dried and then split (using a dry microsplitter) into aliquots containing at least 300 specimens. Each aliquot was counted completely and the counts expressed as percentages of the total number of planktonic foraminifera. The fraction $>125 \mu\text{m}$

VALLE DI MANCHE section

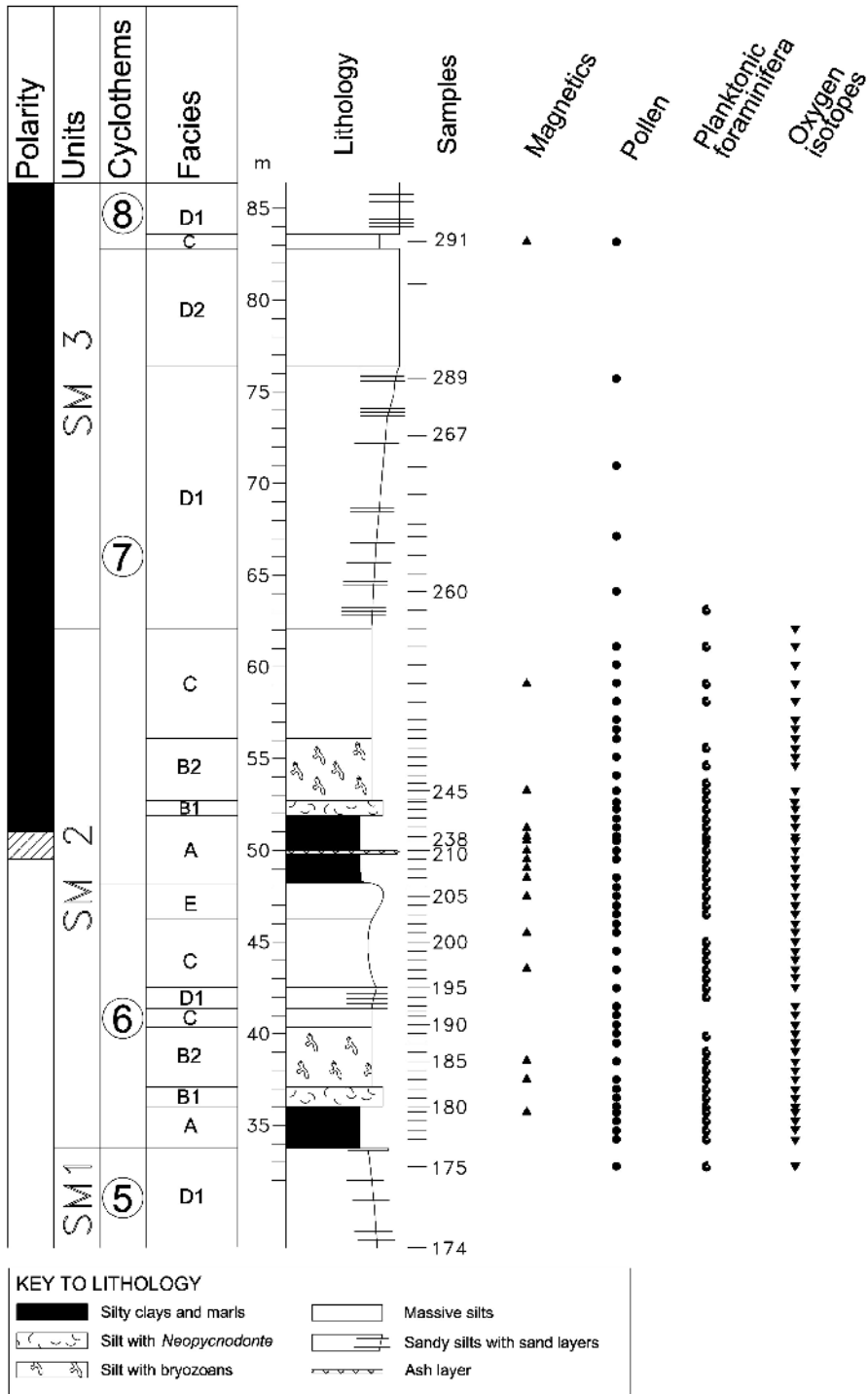


Fig. 4. Columnar log of the Valle di Manche section and location of the analysed samples. See Table 1 for facies description and environmental interpretation.

Table 1. Description and interpretation of the lithofacies

Description and biofabric	Environment
<p><i>Facies A</i> Massive mud (clayey silt, silty clay and locally marl) with dispersed, autochthonous or parautochthonous fauna (<i>Hinia</i>, <i>Funiculina tetragona</i>), <i>Chondrites</i>, <i>Planolites</i> and sparse vegetal debris.</p>	<p>Outer shelf to upper slope. A very rapid deepening trend above the basal surface is attested by foraminiferal assemblages (Poli 1995). The dominant <i>Uvigerina peregrina</i> – <i>Brizalina</i> – <i>Bulimina marginata</i> benthic assemblage suggests fine-grained substrates, high fluxes of organic matter and/or low levels of oxygenation in the interstitial waters.</p>
<p><i>Facies B1</i> Closely spaced firmgrounds mantled by clumps of <i>Neopycnodonte cochlear</i>, an oyster having a gregarious behaviour and forming epibenthic clumps. The shell clusters are true monotypic biogenic concentrations in a matrix of mud, settled on a firm substrate.</p>	<p>The biogenic concentrations represent in-situ epibenthic communities which colonized stiff firmground substrates. Outer-shelf to upper slope palaeodepths are inferred.</p>
<p><i>Facies B2</i> Couplets of alternating lighter, skeletal-rich, overcompacted (firmground) layers of coarse silt and darker, softer, skeletal-poor or barren muddy layers. Layer thickness is in the range of 20–40 cm. The former layers are characterized by a complex cross-cutting of burrows with different degrees of sharpness (including <i>Thalassinoides</i>, <i>Planolites</i>, <i>Teichichmus</i> and <i>Chondrites</i>), and loosely packed, high-diversity skeletal concentrations commonly rich in bryozoans, (<i>Cellaria</i> and <i>Reteporella</i>), associated with fragmentary unsorted skeletal material. The finer-grained layers consist of unconsolidated mud, and, particularly in the upper cyclothem, show a <i>Chondrites</i> ichnocoenosis. This is partly overprinted by burrows of the overlying coarser layer, which appear to pipe downwards. Benthic foraminiferal assemblages indicate a transition from an outer shelf setting (<i>Uvigerina peregrina</i>, <i>Bolivina catanensis</i>, <i>Bulimina marginata</i>, <i>Bulimina costata</i>), to a mid-shelf setting, documented by assemblages dominated by <i>Cassidulina laevigata carinata</i>, associated with <i>Valvulineria bradyana</i>, <i>Cibicidoides</i> and epiphytic forms, such as keeled <i>Elphidium</i> and discorbids, which increase upwards in abundance.</p>	<p>Complex cross-cutting of burrows and sediment consolidation in coarser layers suggest prolonged intervals of minimal deposition, i.e. relative condensation or hiatus; textural features suggest bypassing of suspended load. Intense biogenic reworking reflects episodes of improved benthic oxygenation. Softer layers on the other hand may imply disaerobic conditions.</p>
<p><i>Facies C</i> Massive silty muds with sparse, mostly autochthonous skeletal material (bryozoans, among which are erect fenestrate cheilostomes and cellopiform encrusting forms; molluscs, among which are <i>Isocardia cor</i>, locally with articulated and closed valves, <i>Nucula</i>; sparse echinoids; <i>Ditrupa</i>). The facies is thoroughly bioturbated (<i>Thalassinoides</i>, <i>Planolites</i> and others). Sparse vegetal remains occur with increasing abundance upwards. Benthic foraminiferal assemblages are dominated by <i>Cassidulina</i>, <i>Elphidium</i> and discorbids, associated with <i>Bulimina marginata</i> and <i>Bolivina catanensis</i>.</p>	<p>Middle shelf, grading upwards into a prodelta setting. Fossils in life position suggest a low-energy environment. Siliciclastic sediments are increasingly supplied to the depositional area causing dilution of fossil remains. Preservation of skeletal material may commonly result from burial events due to frequent mud blanketing.</p>
<p><i>Facies D1</i> A variety of this facies occurring in the lower cyclothem is heterolithic and consists of bioturbated mud alternating with erosive-based, planar-laminated, generally thin-bedded tabular to lenticular layers of fine micaceous sand, sometimes normally graded. Stringers of comminuted</p>	<p>Distal to intermediate delta-front, in which suspension-settled background sedimentation is punctuated by sand emplacement by high-energy events, linked to river floods and/or storm-induced flows.</p>

Table 1 continued.

Description and biofabric	Environment
<p>vegetal debris and plant macrorests are extremely abundant. Benthic foraminiferal assemblages are similar to those occurring in facies C.</p> <p>In the upper cyclothem a predominantly massive heavily bioturbated mud to sandy mud with abundant plant debris, <i>Palliolium</i>, <i>Turritella</i>, <i>Chlamys opercularis</i>, <i>Nucula</i>, <i>Dentalium</i> and <i>Ditrupea</i>, grades upwards into a heterolithic bed package, in which the pelitic background facies alternates with sharp- and erosive-based, planar-laminated, thin- to medium-bedded layers of fine to medium sand, commonly micaceous and sometimes normally graded. Sand/mud ratio increases upwards from 1:5 to 1:1. Stringers of comminuted vegetal debris and plant macrorests are abundant, the latter sometimes occurring as nuclei of nodules of Fe-hydroxides (former sulphides). Echinoid burrows may occur near the layer tops. This facies is locally interbedded with sharp-based pavements or stringers (physical concentrations) of disarticulated shells (mostly pectinids and turritellids). Slump scars occur locally.</p>	
<p><i>Facies D2</i> Amalgamated medium- to thick-bedded tabular to broadly lenticular layers of fine to medium sand with planar lamination, sparse echinoid burrows concentrated in upper parts of the layers, and common plant macrorests.</p>	Proximal delta front.
<p><i>Facies E</i> Silt to silty very fine sand with a loosely packed concentration of turritellids, locally associated with sparse pectinids. Benthic foraminiferal assemblages are similar to those occurring in facies C.</p>	Soft-ground biotopes subject to high sedimentation rate in a mid-shelf setting.

was examined for counting. In the interpretation of foraminiferal assemblages, the habitat preferences of the main species of planktonic foraminifera follow Pujol and Vergnaud-Grazzini (1995) and Hemleben *et al.* (1989), and references therein. *Globigerinoides* ex gr. *ruber* comprises *Globigerinoides ruber* (pink and white varieties), *Globigerinoides gomitulus* and *Globigerinoides elongatus*, whereas *Globigerinoides sacculifer* includes the synonyms *Globigerinoides trilobus*, *Globigerinoides quadrilobatus* and *Globigerinoides sacculifer* according to Hemleben *et al.* (1989). The distribution of the main species and groups is reported in Figure 5. We included in 'Other warm water species' (Fig. 5): *Globigerina rubescens*, *Globigerinoides obliquus*, *Globigerinoides tenellus*, *Globigerinoides sacculifer*, *Globigerina praevalida*, *Globigerinella aequilateralis* and *Orbulina universa*. Under 'cold water species' (Fig. 5), *Neogloboquadrina pachyderma*, *Globorotalia scitula*, *Globigerina quinqueloba* and *Globigerina bulboides* are included.

Pollen

A total of 48 samples were processed for pollen analysis (Fig. 4). From each sample, 20 g of sediment were treated according to standard procedures (washing with HCl, soaking in HF for 48 hours, Lüder technique, boiling in diluted KOH) followed by enrichment procedures, in particular heavy liquid separation ($ZnCl_2$ at $d=2.004$), and ultrasound treatment. A tablet containing exotic *Lycopodium* spores was added to each sample in order to calculate the pollen grain concentration within the sediment (Stockmarr 1971). An average of 510 pollen grains and a minimum of 150 were counted in each sample, excluding *Pinus*. Fern and fungal spores and dinoflagellate cysts were not included in the pollen sum. The distribution of selected pollen taxa is presented in Figure 6 and the list of identified taxa is reported in Table 3. A full data set will be submitted to the European Pollen Database and available at http://www.geol.unipd.it/02_personale/home_capra.ro.htm.

Table 2. *Stable isotopes analyses*

Sample	Position (m)	<i>G. ruber</i>			
		<i>G. inflata</i> *		<i>U. peregrina</i>	
		$\delta^{13}\text{C}$	$\delta^{18}\text{O}$	$\delta^{13}\text{C}$	$\delta^{18}\text{O}$
CR92 259	63.10	0.99	1.79	-1.01	3.69
CR92 258	62.10			-0.79	3.51
CR92 257	61.10	0.66	1.98	-0.79	3.62
CR92 256	60.10	1.13	1.45		
CR92 255	59.10	1.04	1.71	-0.67	3.33
CR92 254	58.10	0.97	1.81	-0.50	3.70
CR92 253	57.10	0.96	1.73	-0.52	3.52
CR92 252	56.60	0.80	1.79	-0.29	3.40
CR92 251	56.10	1.31	1.08	-0.36	2.83
CR92 250	55.65	0.96	1.43		
CR92 249	55.10	0.82	1.25	-0.70	2.66
CR92 248	54.65	1.15	1.13	-0.55	2.31
CR92 246	53.65	1.24	0.66		
CR92 245	53.25	1.39	0.42	-0.13	2.48
CR92 244	53.00	1.16	0.06	-0.13	2.38
CR92 243	52.65	1.19	1.25	-0.04	2.58
CR92 242	52.25	1.10	-0.40	-0.45	2.04
CR92 241	51.75	1.16	-0.63	-0.57	2.08
CR92 240	51.25	1.07	-0.92	-0.49	1.99
CR92 239	50.75	0.54	-0.02	-0.83	2.03
CR92 238	50.50	0.78	-0.32	-0.72	2.25
CR92 210	50.00	0.61	-0.20	-1.19	2.41
CR92 209	49.50	0.90	-0.77	-1.05	2.33
CR92 208	49.00	0.80	-0.36	-1.22	2.28
CR92 207	48.50	0.84	-0.07	-1.51	2.23
CR92 206	48.00			-0.63	2.48
CR92 205	47.50	0.28	2.44	-0.35	2.78
CR92 204	47.00	-0.01	2.34	-0.70	2.88
CR92 203	46.50	0.25	2.31	-0.46	2.73
CR92 202	46.00	0.22	2.37		
CR92 201	45.50			-0.31	3.11
CR92 200	45.00	0.03	3.14		
CR92 199	44.50	-0.06	2.88	-1.14	3.44
CR92 198	44.00	-0.09	2.84	-0.34	3.43
CR92 197	43.50	0.09	2.75	-1.04	3.18
CR92 195	42.50	0.01	3.18	-1.11	3.43
CR92 193	41.50			-0.56	4.10
CR92 191	41.00	0.96	1.43	-0.27	3.84
CR92 190	40.50	1.09	2.00	-0.16	3.67
CR92 189	40.00	0.84	1.79	-0.28	3.66
CR92 188	39.75	0.60	1.86	-0.23	3.85
CR92 187	39.50	0.63	1.67	-0.19	3.99
CR92 186	39.00	1.06	1.89	-0.47	3.57
CR92 185	38.50	1.26	1.50	-0.36	3.59
CR92 184	38.00	0.59	1.78	-0.25	3.23
CR92 183	37.50	0.62	1.58	-0.26	3.57
CR92 182	37.00	1.06	0.14	-0.25	2.59
CR92 181	36.50	0.90	0.51	-0.50	2.41
CR92 180	36.05	0.93	0.17	-0.15	2.00
CR92 179	35.75	0.85	-0.27	-0.55	1.97
CR92 178	35.25	0.99	-0.64	-0.48	2.22
CR92 177	34.75	0.41	0.05	-0.26	2.37
CR92 176	34.25			-0.30	3.10
CR92 175	32.75	0.40	1.53	-0.47	3.71

**G. inflata* data in bold italic typeface.

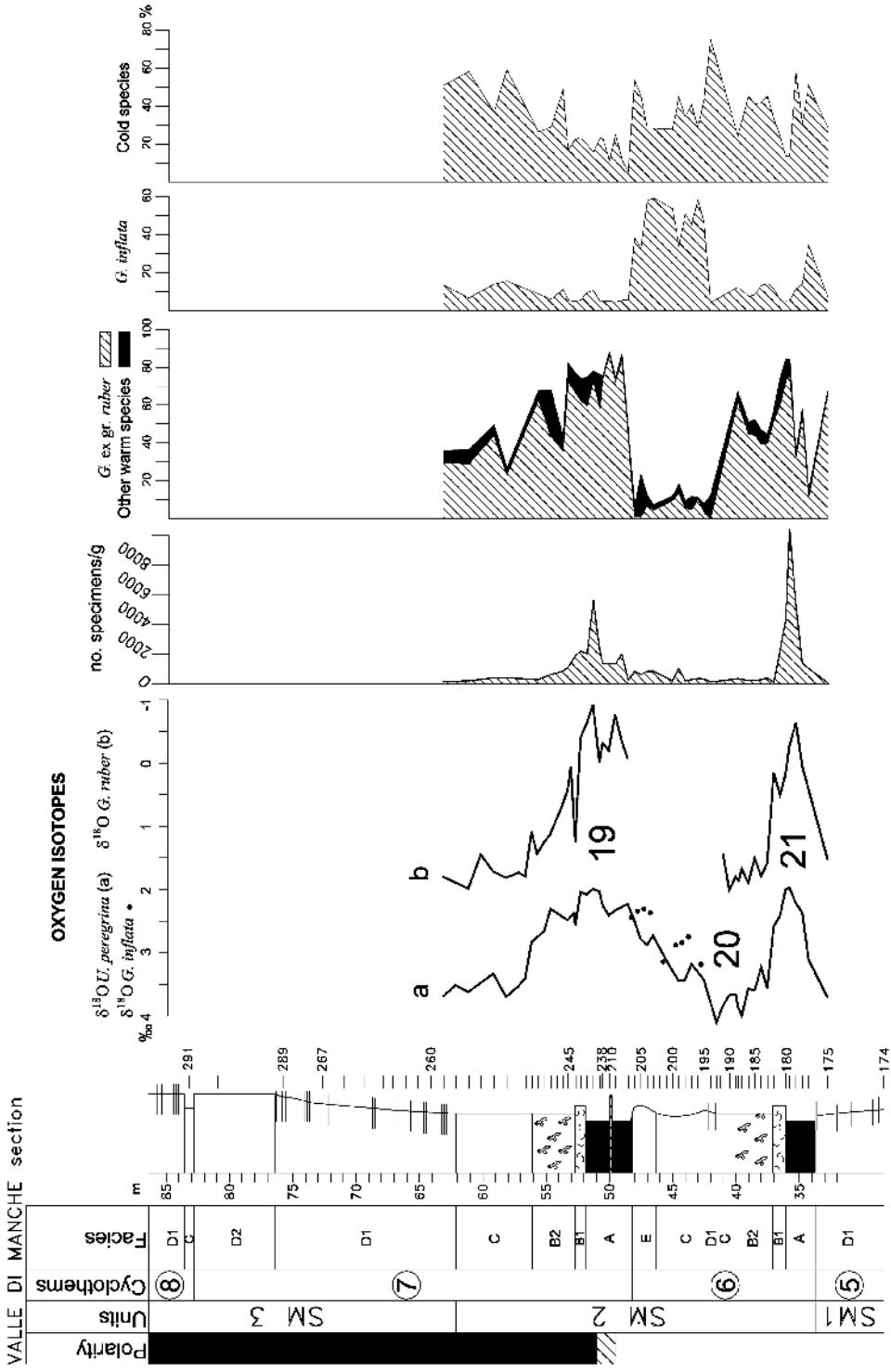


Fig. 5. Results of the Valle di Manche section. Left: stable oxygen isotope ratio ($\delta^{18}\text{O}$) performed on the benthic foraminifera *Uvigerina peregriana* and planktonic foraminifera *Globobulimina ruber* and *Globobulimina inflata*. Right: relative abundance of ecologically significant groups of selected planktonic foraminifera. See Figure 4 for key to lithology.

Table 3. Simplified checklist of the recognized pollen taxa

Trees (AP)		Herbs (NAP)	
Pollen type	Ecological group	Pollen type	Ecological group
<i>Pinus diploxylon</i> -type <i>Pinus haploxylon</i> -type <i>Pinus</i> > 100 mm	<i>Pinus</i> (removed)	<i>Ephedra</i> (2 types) <i>Artemisia</i> Chenopodiaceae <i>Erodium</i> <i>Armeria</i> <i>Limonium</i>	Steppic and halophytic plants
<i>Abies</i> (2 types) <i>Picea</i> (2 types) <i>Fagus</i> (2 types) <i>Betula</i>	Mountain ('alpine') elements (<i>Picea-Abies</i> group)	Asteraceae cf. Cichorioideae Asteraceae cf. Asteroideae <i>Centaurea</i> Boraginaceae Caryophyllaceae Cistaceae Brassicaceae Dipsacaceae Ericaceae Gentianaceae Geraniaceae Poaceae Lamiaceae Fabaceae Linaceae Malvaceae Plantaginaceae Ranunculaceae <i>Thalictrum</i> Rubiaceae Apiaceae Liliflorae Papaveraceae Valerianaceae Primulaceae Rosaceae Saxifragaceae <i>Epilobium</i> Obligate water plants (4 types)	NAP (cosmopolitan herbs)
<i>Quercus ilex/coccifera</i> -type Oleaceae <i>Olea</i> <i>Phillyrea</i> <i>Pistacia</i> <i>Rhus</i> <i>Ilex</i> <i>Buxus</i> Lauraceae Myrtaceae <i>Quercus</i> (deciduous) <i>Corylus</i> <i>Carpinus</i> cf. <i>betulus</i> <i>Carpinus</i> cf. <i>orientalis</i> <i>Ostrya</i> <i>Castanea</i> Ulmaceae <i>Ulmus</i> <i>Zelkova</i> <i>Celtis</i> Juglandaceae <i>Juglans</i> <i>Carya</i> <i>Pterocarya</i> (2 types) <i>Engelhardtia</i> <i>Platycarya</i> cf. <i>Hamamelis</i> cf. <i>Parrotia</i> <i>Liquidambar</i> <i>Fraxinus</i> <i>Tilia</i> <i>Vitis</i>	Mediterranean evergreen elements Mesic elements (deciduous temperate forest)		
<i>Taxus</i> Cupressaceae <i>Alnus</i> <i>Salix</i> <i>Populus</i>	Other trees (riparian and ubiquitous species)		
<i>Cedrus</i> <i>Tsuga</i> cf. <i>canadensis</i> <i>Tsuga</i> cf. <i>diversifolia</i>	<i>Tsuga-Cedrus</i> group		

The oxygen isotope stratigraphy

The oxygen isotope records of foraminiferal calcite in marine sediments provide a highly resolved standard reference for Pleistocene chronology as well as critical palaeoenvironmental information. Oxygen isotope data from benthic foraminifera are widely used as a proxy for eustatic variations in spite of the numerous uncertainties remaining in linking relative sea level (RSL) changes to the differential $\delta^{18}\text{O}$ ice volume (Waelbroek *et al.* 2002). The Mediterranean Sea is a concentration basin and the oxygen isotope records in both planktonic and benthic foraminifera are affected by strong regional overprints related to local salinity (evaporation–precipitation), temperature and circulation (Vergnaud Grazzini *et al.* 1977). However, numerous previous (mainly planktonic) records indicate a good correlation between Mediterranean and oceanic isotopic records, thus suggesting that global ice volume fluctuations are a primary controlling factor on the oxygen isotope composition of Mediterranean foraminiferal calcite. Indeed, the following discussion (Fig. 5 and Table 2) indicates that, in spite of the shelfal setting, the $\delta^{18}\text{O}$ variations detected in the Valle di Manche section seem to correlate with the standard global MIS (Fig. 7).

The benthic record

The $\delta^{18}\text{O}$ of *U. peregrina* varies from 4.10‰ to 1.97‰ (Table 2). The lightest values (*c.* 2‰) correspond with fine lithologies (Facies A) of the two cyclothems (Fig. 5). They compare well with the isotopic composition of modern *Uvigerina* spp. in the eastern Mediterranean which varies from 1.80‰ (Sicilian Strait) to 2.20‰ (off Israel), with an average value of 2.14‰ (Vergnaud Grazzini *et al.* 1986). We interpret $\delta^{18}\text{O}$ values for *U. peregrina* of about 2.0‰ as reflecting interglacial conditions (Fig. 5). The heaviest values of *U. peregrina* are about 4‰. We consider values in excess of 3.5‰ as indicative of glacial conditions in this depositional setting. There are few isotopic data on benthic foraminifera from the Mediterranean during the Pleistocene. Vergnaud Grazzini *et al.* (1986) reported values ranging from 4.9‰ to 4.25‰ for *Uvigerina* spp. for various water masses during the last glacial maximum. The benthic values in our samples reflect bottom water temperatures on the continental shelf, and are not comparable with coeval temperatures in the deep-sea environment. The maximum $\delta^{18}\text{O}$ amplitude shown by *U. peregrina* is 2.13‰. This exceeds the approximately 1.5‰ variation observed in deep-sea sediments that is considered to chiefly reflect global ice volume (Shackleton & Opdyke 1973).

The planktonic record

The variation in $\delta^{18}\text{O}$ for the surface dweller *Globigerinoides ruber*, where available, largely follows that of *U. peregrina* (Fig. 5). Most of the $\delta^{18}\text{O}$ shifts appear nearly synchronous in both records. The oxygen isotopic composition of modern *G. ruber* in the Mediterranean displays a decreasing trend when passing from the western (+0.64‰) to the eastern (−1.04‰, off Israel) basins, reflecting the temperature gradients from western to eastern basins (Vergnaud Grazzini *et al.* 1986). In the Ionian Sea, intermediate values are found (−0.83‰ $\delta^{18}\text{O}$) that compare well with the lightest values observed (−0.92‰) in the Valle di Manche section. The heaviest recorded value is +2.0‰. The glacial–interglacial $\delta^{18}\text{O}$ range is 2.92‰. This value is close to an average range of 2.9‰ observed between the Holocene and the last glacial maximum for the eastern Mediterranean (Thunell & Williams 1989). In the Ionian Sea core KC01B (Langereis *et al.* 1997; Rossignol-Strick & Pateme 1999; Fig. 1), the $\delta^{18}\text{O}$ of *G. ruber* varies from +2.35 to −0.82‰ (maximum amplitude of 3.17‰) in the interval correlative with the Valle di Manche section (Fig. 7). These larger ranges in Pleistocene isotopic amplitudes probably reflect the unique set of evaporation–precipitation and temperature conditions in the Mediterranean.

In the interval where *G. ruber* is not available (41 to 48 m) we have used *Globorotalia inflata* to obtain $\delta^{18}\text{O}$ values varying from 3.18‰ to 2.31‰ (Table 2 & Fig. 5). *Globorotalia inflata* is a mesopelagic form that in the Mediterranean mainly grows during the late winter season when the structure of the water mass is generally homogeneous (Pujol & Vergnaud Grazzini 1995), and calcifies its test over a wide range of water depths (Vergnaud Grazzini *et al.* 1986). These authors showed that, in the Mediterranean, the isotopic gradient between the surface-dwelling *G. ruber* and the deep-dwelling *G. inflata* is strong during interglacials and decreases to near zero during glacial maxima. For this reason, we did not correct the *G. inflata* values to simulate a continuous planktonic record. However, the $\delta^{18}\text{O}$ values of *G. inflata* are parallel or very close to those of *U. peregrina* (Fig. 5), with a gradient between these two species of 0.04 to 0.59‰.

Correlation to standard marine isotope stratigraphy

The two $\delta^{18}\text{O}$ records from the Valle di Manche section show two interglacial intervals that correspond with the fine lithologies of Facies A (Fig. 5). Considering the available biomagnetostratigraphic constraints in the section, it seems straightforward to correlate these two interglacial intervals with MIS

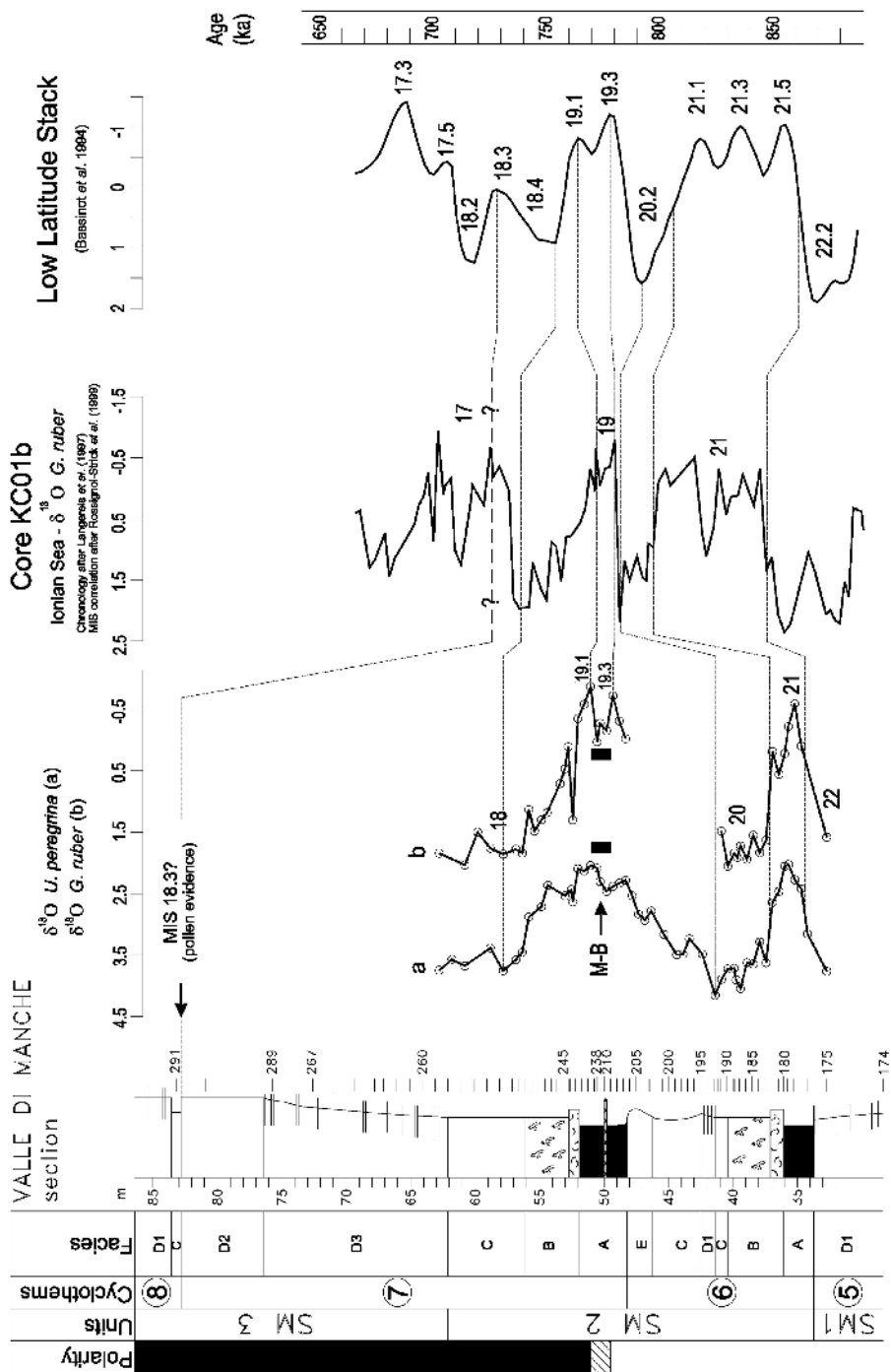


Fig. 7. Comparison between the $\delta^{18}O$ records of the Valle di Manche section (sample position is given in thickness) and the age-tuned Core KC01b and Low Latitude Stack. Dashed lines indicate the correlation points used. Note that MIS 18.3 of Bassinet *et al.* (1994) is apparently missing in Core KC01b, where isotope substages have not been recognized so far (Langeris *et al.*, 1997; Rossignol-Strick & Pateme 1999). M-B, Matuyama-Brunhes boundary and relative uncertainty interval (thick solid line). See Figure 4 for key to lithology.

VALLE DI MANCHE section

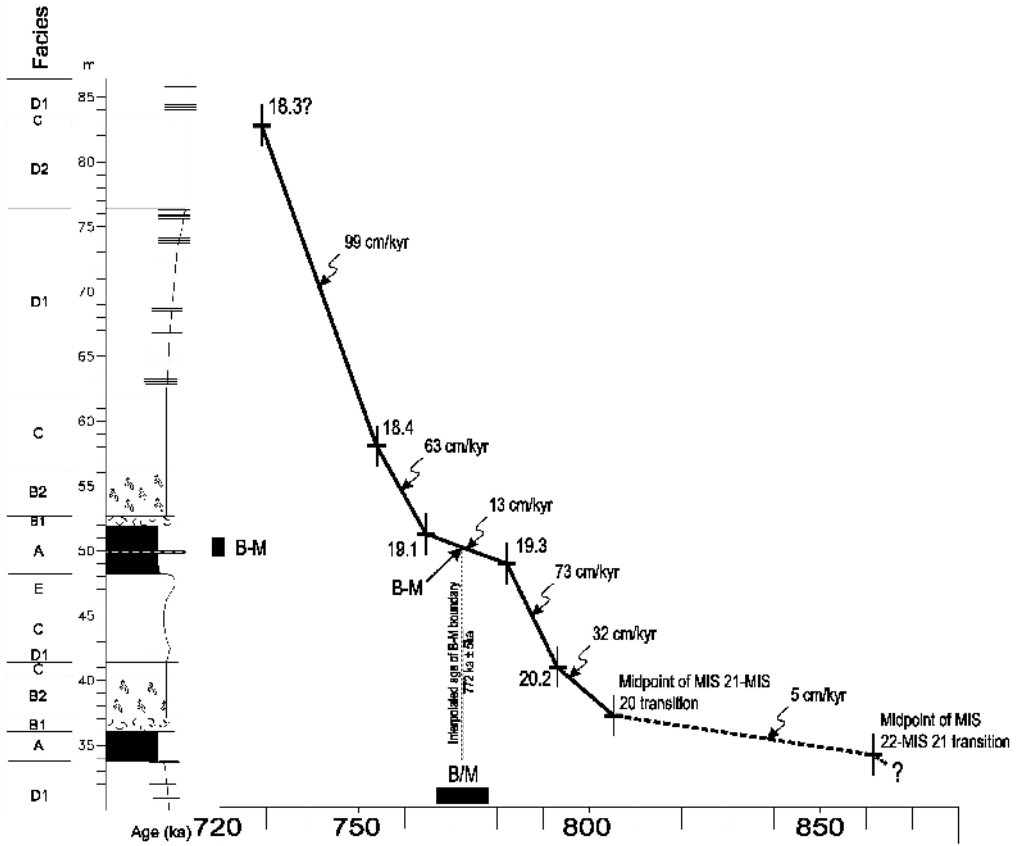


Fig. 8. Calculated sedimentation rates in the Valle di Manche section. Standard MIS labels for age control points (after Bassinot *et al.* 1994) are also shown. M-B, Matuyama-Brunhes boundary and relative uncertainty interval (thick solid line). See Figure 4 for key to lithology.

21 and MIS 19, in agreement with the previous suggestion of Rio *et al.* (1996; Fig. 2). In Figure 7, we compare the isotope records of the Valle di Manche section with the *G. ruber* record of Core KC01b and with the low-latitude stack of Bassinot *et al.* (1994) in order to derive a more resolved chronology for the section. From this comparison, it is apparent that the three substages of MIS 21 are not resolved in our record. This may be because of an inadequate sampling resolution in the interval, or it may be due to millennial-scale hiatuses related to sea level variations in this shallow-water setting. The transitions from MIS 20 to MIS 19, and MIS 19, are both expanded, possibly relating to increasing tectonic subsidence producing an increase in accommodation space and sediment accumulation rates. The interglacial MIS 19 shows variability although it is impossible to recognize MIS substages 19.1 and 19.3 in the benthic record. In contrast, the *G. ruber*

$\delta^{18}\text{O}$ records from the Valle di Manche section and in core KC01b from the Ionian Sea both show recognizable isotope substages within MIS 19 (Fig. 7), and are thus correlatable at substage level. Based on the correlations indicated in Figure 7, we have derived the age control points reported in Table 4 and constructed the sediment accumulation rates shown in Figure 8. We have used the astronomical chronology of Bassinot *et al.* (1994), which differs from that established in Core KC01b by Langereis *et al.* (1997) on the basis of Mediterranean sapropels. But whatever chronology is used, sediment accumulation rates are highly variable (Fig. 8). There is a general increase in sediment accumulation rates upwards in the section in agreement with the fact that cyclothem 6 is about 13.5 m thick, whereas cyclothem 7 is 34.7 m thick. There is also an overall agreement with the facies distribution. The reduced sediment accumulation rates correspond to the fine

Table 4. Age control points

Correlation points (standard oxygen stratigraphy)	Position (m)	Age (ka)	
		Sapropel chronology*	Low-latitude stack†
MIS 17.5	82.80	725	708
MIS 18.2	61.10	740	718
MIS 18.4	58.10	750	754
MIS 19.1	51.25	772	765
MIS 19.3	49.00	780	782
MIS 20.2	41.00	783	793
MIS 21.1	35.75	808	820

*Langereis *et al.* (1997).†Bassinot *et al.* (1994).

sediments of Facies A (MIS 19) and the increased rates to the coarse-grained sediments of Facies D. The proposed age model shows that, for pollen analysis, a mean sample resolution of *c.* 1 ka was attained during the transition from MIS 20 to MIS 19 and during the transition from MIS 19 to MIS 18.4. Lower sampling resolutions are available at the MIS 18.4–18.3 transition (2.8 ka) and in the MIS 19.3–19.1 interval (3.4 ka).

Planktonic foraminifera

In the Valle di Manche section, the planktonic foraminifera are reasonably well represented only in cyclothem 6 and in the lower part (up to *c.* 64 m) of cyclothem 7. Their concentration is plotted in Figure 5 as the number of specimens per gram. The concentration of planktonic foraminifera sharply increases with the appearance of Facies A sediments, interpreted as representing condensed intervals (Massari *et al.* 2002). The oxygen isotope data presented in Figure 5 indicate that this facies represents maximum sea level stands.

Interglacials (MIS 19 and MIS 21)

The full interglacial conditions (MIS 21 and 19) are characterized by relatively high percentages of warm-water species (mainly *Globigerinoides ex gr. ruber*, up to 75%) and relatively low percentages of cold-water species, including *Globorotalia inflata*. The subtropical species *G. ex gr. ruber* lives today in warm and oligotrophic surface waters of the Mediterranean where it is prolific at the end of summer, preferring well-stratified waters (Pujol & Vergnaud Grazzini 1995). *Globorotalia inflata* is a herbivorous species that proliferates during winter in the modern western Mediterranean (Pujol &

Vergnaud Grazzini 1995; Hemleben *et al.* 1989). High percentages of this species occur when the thermocline is eliminated and the water column becomes homogeneous. The assemblage in the Valle di Manche section suggests that MIS 19 and MIS 21 were characterized by a relatively long season with warm, stratified and oligotrophic surface waters and reduced vertical mixing during winter. Moreover, the near-absence of herbivorous species, such as *G. inflata* and *Neogloboquadrina*, and the low percentage of species related to high nutrient levels (*Globigerina quinqueloba* and *Globigerina bulloides*), indicate low productivity in the waters throughout the year.

Glacials (MIS 20 and MIS 18)

These intervals show a general increase of cold-water species, while *Globorotalia inflata* shows low percentages (below 10%). A relatively high surface productivity is inferred during the late phase of MIS 20 from the increase of *Globigerina quinqueloba* (reaching 47%), but the winter vertical mixing must have been weak, as indicated from the low abundance of *G. inflata*. The main character of these glacial intervals is the relatively high abundance of warm water species (mean values of *c.* 40%; see Fig. 5), indicating relatively mild conditions. During the early phase of MIS 18, *Globigerinoides ex gr. ruber* displays an increasing trend from 38.5 m culminating with high percentages (62%) at about 39.85 m. This spike corresponds to heavy oxygen-isotope values. A similar feature can also be recognized during MIS 18 in Ionian core KC01b (Sanvoisin *et al.* 1993), as well as in other glacial intervals, such as MIS 2, in the central Mediterranean (Sbaffi *et al.* 1998, 2001; Capotondi *et al.* 1999). Sbaffi *et al.* (2001) interpreted this feature as a warming event within MIS 2. This may indicate relatively warm waters accompa-

nied by an increase in surface water salinity, because *G. ruber* can tolerate changes in salinity of up to 49% (Hemleben *et al.* 1989; Bijima *et al.* 1990).

Deglaciation (MIS 20–MIS 19 transition)

The expanded transition (deglaciation) from MIS 20 to MIS 19 is dominated by *Globorotalia inflata* (up to 50%) and *Globigerina quinqueloba*, whereas the warm water taxa decrease below 10%. This assemblage points to waters colder than in the underlying MIS 20 glacial interval, and to high productivity conditions, because of the dominance of herbivorous species, such as *G. inflata*, *G. quinqueloba* and *N. pachyderma*. The high frequency of *G. inflata* suggests the presence of strong vertical mixing during the winter. In addition, according to Pujol & Vergnaud Grazzini (1995, and references therein), *G. inflata* generally occurs only in the western Mediterranean in areas that coincide with the path of both Modified Atlantic Waters (MAW) and Levantine Intermediate Waters (LIW). Hydrographic circulation in the Mediterranean basin is controlled by water exchange with the Atlantic. Surface inflow, 100–200 m deep, of less saline North Atlantic Waters (NAW), can be traced as far as the eastern Mediterranean. A subsurface outflow, at between 200 and 600 m depth, of relatively more saline Mediterranean waters comprising mostly LIW, forms in the eastern Levantine Basin during winter (Armi & Farmer 1985; Bryden & Kinder 1991). The high frequency of the 'western' species *G. inflata* in the Ionian basin suggests a palaeoceanographic setting different from the modern one and more similar to the modern western Mediterranean. Consequently, we can infer a relatively higher flux of MAW into the eastern Mediterranean. This condition has also been recorded during the two-step deglaciation of the Last Termination by relatively high abundance of *G. inflata* both in the Ionian basin (Hayes *et al.* 1999) and in part of the Adriatic Sea (Jorissen *et al.* 1993; Capotondi *et al.* 1999; Asioli *et al.* 2001).

Pollen

All 48 processed samples contain moderately to well preserved pollen. The concentration of arboreal plant (AP) pollen varies from 870 to 10 000 grains per gram (Fig. 6). Higher concentrations are observed in the full glacial intervals of MIS 20 and 18, where a three-fold increase dominated by the high abundance of *Pinus* is observed (Fig. 6). The pollen assemblages are dominated by *Pinus* spp., which account for 40–85% of the total floral assemblage. Several different morphotypes of *Pinus* are present. The presence of larger-sized pine grains,

which are characteristic of Mediterranean-type pines (Van Campo-Duplan 1950; Accorsi *et al.* 1978), and the presence of *Pinus haploxylon* (mostly *Cathaya* according to Suc 1976) are noteworthy. The abundance of *Pinus* in marine sediments is related to taphonomy (better transport and better preservation), implying that its climatic meaning is difficult to interpret and therefore, following a well established practice (e.g. Comburieu-Nebout 1987), the pollen percentages in Figure 6 are calculated excluding this taxon. However, because *Pinus haploxylon* was considered in the past as having biostratigraphic significance (Bertoldi 1977), its relative abundance is reported in Figure 6.

Composition of the flora

The relative abundance of selected major pollen taxa is shown in Figure 6. The general make-up of the retrieved pollen assemblage is similar to the modern flora of southern Italy and clearly reflects the presence of variable vegetation belts in the borderland during the time interval recorded in the Valle di Manche section. A total of 85 pollen taxa were observed, as presented in Table 3, where pollen are split into vegetation groups according to the present-day distribution and ecology of reference plants. AP and non-arboreal plants (NAP) are present over the entire sequence with variable relative abundance. The AP group includes Mediterranean evergreen elements (e.g. *Quercus ilex*-type, *Olea*, *Phillyrea*, *Pistacia*), deciduous forest trees (e.g. *Quercus*, *Corylus*, *Carpinus*, *Ulmus*) and mountain elements (mainly *Abies* and *Picea*, with sporadic *Betula* and *Fagus*). With respect to present-day vegetation, it is noteworthy that the mountain belt was apparently dominated by species of *Abies* and *Picea* (Fig. 6), whereas presently it is dominated by *Fagus* (Gellini & Grossoni 1997). Therefore, the recovered *Picea*–*Abies*–*Fagus* fossil assemblage points to an alpine-type forest rather than to the present-day Mediterranean mountain belt. In addition, besides *Pinus haploxylon*-type pollen, low abundances of other taxa presently exotic for both Italy and Europe are present (*Tsuga*, *Cedrus*, *Hamamelis*, *Liquidambar*, *Carya*, *Pterocarya*, *Engelhardia*–*Platycarya*). Among the NAP group, both cosmopolitan herbs (Asteraceae, Poaceae and less meaningful taxa) and steppic plants (*Artemisia*, *Ephedra*, Chenopodiaceae and *Erodium*) are consistently present.

Pollen zones and climatic interpretation

The pollen assemblages have been subdivided into five ecological groups (Table 3) according to the present-day organization of vegetation belts in

VALLE DI MANCHE section

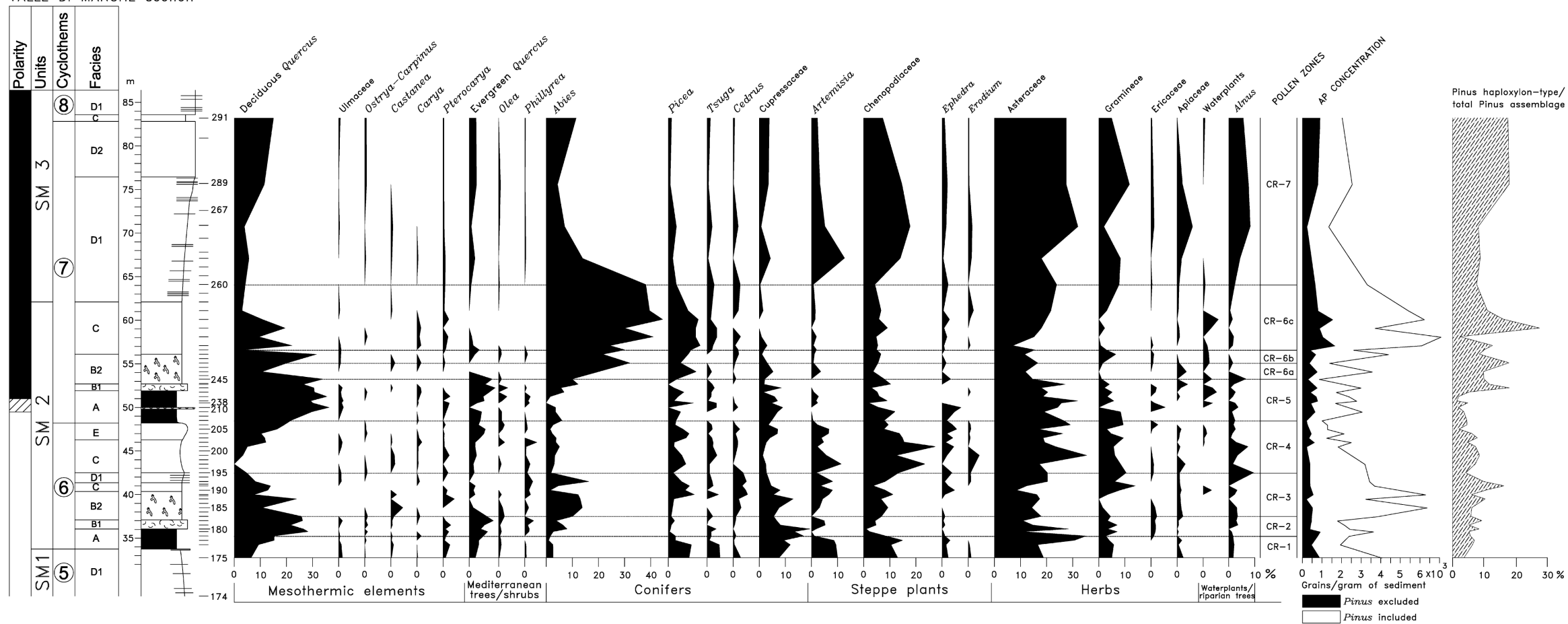


Fig. 6. Relative abundance of selected pollen taxa calculated without *Pinus*. AP concentration, pollen density (no. specimens/g) calculated from pollen of total arboreal plants (AP). Far right: relative percentage distribution of *Pinus* subgen. *haploxylon* with respect to the total *Pinus* assemblage. See Figure 4 for key to lithology.

southern Italy (Fig. 3). Although the major vegetation groups are present to some extent throughout the sequence (Fig. 9), the studied section can be subdivided into seven pollen assemblage zones (PAZ) that are defined by alternating peaks of different groups as summarized in Table 5. Each zone is interpreted as reflecting the different developments of vegetation belts in the surrounding areas in response to changing environmental and, especially, palaeoclimatic conditions. The palynostratigraphy obtained points to a rhythmic alternation in the regional vegetation, that oscillates between three principal states: (1) a forested state dominated by mesothermic elements, (2) a forested state dominated by alpine elements (*Picea-Abies*), and (3) a wooded steppe state. However, a closer inspection of the record reveals that each of the principal vegetation states has been highly variable.

Mesothermic (mixed oak) forest. Major developments of mesothermic forest and the concomitant decline of NAP and alpine forest (*Picea* and *Abies*) characterize Zones CR-2 and CR-5 (Fig. 9). This appears to reflect a forested landscape rich in both Mediterranean evergreen and deciduous broad-leaved trees (mainly oaks) similar to the modern Mediterranean and Sannitic vegetation belts in Calabria (Fig. 3). The dominant vegetation may have comprised tall evergreen shrubs (maquis) and trees of the coastal area, gradually transforming into a closed deciduous forest on the surrounding hills and mountain slopes. As at present, water-demanding evergreen trees (*Abies*, *Picea* and secondarily *Tsuga* and *Cedrus*) survived most probably on the milder mountain peaks and valleys. In spite of floristic differences, the climatic conditions during these intervals appear quite similar to the present interglacial. In fact, a pronounced seasonality with warm, dry summers and mild, cool winters and an average rainfall of about 600–700 mm/a, mainly concentrated during winter, is indicated.

Mountain (alpine) forest. Following the mesothermic forest intervals (Zones CR-2 and CR-5), forested conditions persist in both cyclothem 6 and 7. However, in both cases the mesothermic forest decline, and a massive expansion of the mountain ('alpine') elements (*Picea-Abies* group) is observed in parallel with a gradual increase in NAP (Zones CR-3 and CR-6 in Fig. 9). The abundance of *Abies* and *Picea* can be explained both by a downward shift of the mountain vegetation and by an enhanced fluvial transport of pollen from higher altitudes. However, because of the evidence of persisting Mediterranean and deciduous forests, a coastal landscape dominated by fir and spruce is quite unrealistic. The increasing percentages of the *Picea-Abies* group correspond to a pronounced decrease of the broad-

leaved forest and, hence, we prefer to envisage a coniferous forest massively and gradually invading the former Sannitic belt. This vegetation turnover suggests a reduction in average temperature concomitant with a major enhancement of precipitation. We assume an annual average rainfall largely in excess of 1200 mm per year that becomes non-seasonal and therefore regularly distributed during the year. In the expanded cyclothem 7, the early part of the alpine forest state is characterized by strong instability that allows the subdivision of Zone CR-6 into three sub-zones (6a, 6b and 6c; Fig. 9) based on significant increases of mesothermic elements (mainly deciduous trees) at the expense of mountain elements.

Wooded steppe. Zones CR-1, CR-4 and CR-7 are characterized by the dominance of NAP over arboreal taxa, mainly represented by pines. Zone CR-1 is poorly developed and poorly documented. Zones CR-4 and CR-5 are expanded and bounded by alpine forest below and mesothermic forest above (Fig. 9). Within the NAP, steppe elements (*Artemisia*, *Ephedra*, Chenopodiaceae) are well represented and in most instances account for half of the total NAP assemblage (Fig. 9). Forest elements are also significant in Zones CR-4 and CR-7. Hence, we envisage a wooded steppe ('parkland') landscape with water-demanding trees (*Picea*, *Abies* and mesothermic elements) restricted to favourable areas with patches of resistant trees (mostly pines) surviving in lowland areas.

Taxonomic determinations at species level are not possible for most of the herbaceous pollen types and, hence, the prevailing temperature regime cannot be defined. Indeed, similar xeric assemblages can be associated with both warm and cold regimes (Follieri *et al.* 1988). However, the high percentage values of vegetation dominated by NAP (over 50% of the total floral assemblage) indicate a reduced annual precipitation rate (Quézel *et al.* 1980) and point to the most arid conditions observed in the section.

Vegetation cycles and MIS

The Valle di Manche section contains a predictable large-scale repetition of the main vegetation states (mesothermic forest, mountain forest, wooded steppe) indicating a climate-driven, cyclic influence in the observed changes in vegetation. Specifically, vegetation conditions similar to those of today (Zones CR-2, CR-5 and CR-6b) are followed by an expansion of the mountain belt (Zones CR-3, CR-6a, CR-6c) and, finally, by the establishment of a wooded steppe (CR-4 and CR7). We recognize two complete vegetation cycles, which are coherent with the physical stratigraphy, and data provided by planktonic foraminifera and oxygen isotopes. Comparison of the pollen data with oxygen isotope

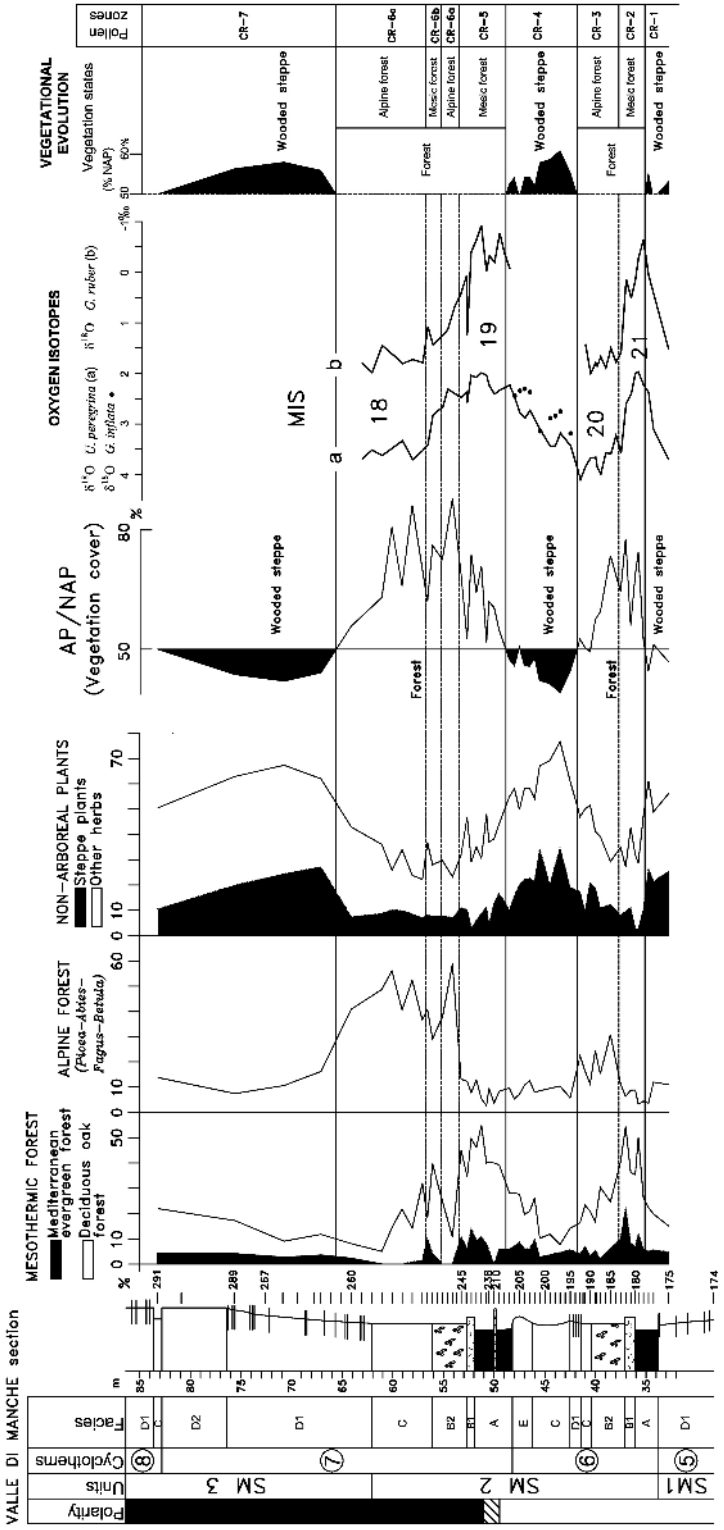


Fig. 9. Comparison between pollen (excluding *Pinus*) and oxygen isotope data in the Valle di Manche section. Left: relative distribution of significant ecological groups that indicate variable climatic conditions with respect to the present day. Middle: AP/NAP ratio, which gives information about the vegetation cover (extent of woodlands and forests) strictly related to annual average precipitation. Right: subdivision of the pollen record into pollen assemblage zones (PAZ) according to changing vegetation states. See Figure 4 for key to lithology.

Table 5. *Pollen zones recognized and interpreted climatic evolution*

Pollen assemblage zones (PAZ) and relative boundaries (m)	Vegetation features	Interpreted climate	Correlative MIS
CR-7 64.10–83.20	NAP are dominant. AP percentages are low, although they increase towards the top. Non-forested environment.	Very dry to arid climate. Precipitation is irregularly scattered throughout the year.	MIS 18.4 to >MIS 18.3
CR-6c 56.60–64.10	Forested environment dominated by mountain conifers. Oak forest declines and NAP percentages remain low.	Cool to cold climate characterized by abundant precipitation throughout the year (low seasonality).	MIS 18.4
CR-6b 55.10–56.60	Forested environment dominated by broad-leaved trees. Mountain conifers decline and NAP are poorly represented.	Similar to present day. Mild temperatures and seasonal regime of precipitation.	?
CR-6a 53.25–55.10	Forested environment dominated by mountain conifers. Oak forest and herb communities collapse.	Cool to cold climate characterized by abundant precipitation throughout the year (low seasonality).	MIS 19 to >18?
CR-5 48.50–53.25	Sharp rise in mesic assemblage. Both NAP and mountain elements decline. Forested environment dominated by oaks.	Similar to present day. Mild temperatures and seasonal regime of precipitation.	19
CR-4 42.50–48.50	Re-establishment of a non-forested environment, during which both AP groups collapse. Steppe-like vegetation.	Very dry to arid climate. Precipitation is irregularly scattered throughout the year.	MIS 20 to >MIS 19
CR-3 37.50–42.50	Sharp increase in mountain conifers. Broad-leaved trees and NAP decline. Forested environment dominated by mountain conifers.	Cool to cold climate characterized by abundant precipitation throughout the year (low seasonality).	MIS 20
CR-2 32.75–37.50	Rising of a dominant broad-leaved trees community, whilst NAP concomitantly decline. Forested environment dominated by oaks.	Similar to present day. Mild temperatures and seasonal regime of precipitation.	MIS 21
CR-1 32.75–35.75	NAP percentages reach up to 70% of total pollen assemblage. Steppe-like environment.	Very dry to arid climate. Precipitation is irregularly scattered throughout the year.	MIS 22 to >MIS 21

stratigraphy (Fig. 9) indicates that the mesothermic forest states correspond to the full interglacial conditions of MIS 21 and 19. Surprisingly, the full glacial condition of MIS 20 and MIS 18 corresponds to alpine forest states. This is unexpected because, in the central Mediterranean area, it is thought that since Middle Pliocene (Piacenzian) times (e.g. Bertini 2001), the glacial intervals were characterized by arid conditions leading to dominance of

steppe vegetation. Our direct oxygen isotope–pollen correlation (Fig. 9) indicates that, in the examined time interval, the most arid conditions occurred at glacial terminations. At the onset of glacial terminations the NAP group reaches its maximum value and then decreases, thus pointing to a stepped forestation of the landscape. It must be stressed that a genuine steppe environment cannot be envisaged on the basis of our data for the time interval examined in this part

of the central Mediterranean, in contrast to the observations of Tzedakis *et al.* (1997) for the last 500 ka. We note also that it is premature to conclude that the forested conditions observed during MIS 20 and 18 apply to other Early Pleistocene glacial intervals in the central Mediterranean. Nevertheless, the results confirm that steppe and/or arid conditions should not be equated with glacial maxima without independent supporting evidence.

The chronology in the upper part of the section

The upper part of the Valle di Manche section (from c. 64 m to the top) lacks any marine chronological control due to the unfavourable facies (Fig. 4 and Table 1). However, pollen are well represented and indicate an expanded wooded steppe phase (PAZ CR-7) that follows the alpine forest phase of CR-6c, correlated to MIS 18 (Fig. 9). PAZ CR-7 shows a trend identical to that of PAZ CR-4 that can be correlated with the MIS 20 to MIS 19 deglaciation (Fig. 9). We therefore conclude that PAZ CR-7 may represent with the deglaciation associated with MIS substage 18.3. This substage is well developed in most $\delta^{18}\text{O}$ records published to date (see Channell & Kleiven 2000, fig. 2). Our correlation is coherent with the character of the physical stratigraphy. The presence of a package of fine sediments (Facies C) has been interpreted as a transgressive surface (Massari *et al.* 2002) at the top of PAZ CR-7, consistent with the potential deglaciation.

Long-term evolution of flora in the central Mediterranean

This paper opens a well constrained time window on the evolution of vegetation and flora in the central Mediterranean from c. 0.9 to c. 0.7 Ma, i.e. from the later Early Pleistocene to the basal Middle Pleistocene. How do these results compare to others? A full and detailed reply to this question is not possible because only a few well dated records are available to date, as shown by Bertini (2003) in a recent review of the Pleistocene pollen records in Italy. Most of the available records have been recovered from continental successions, where rigorous chronological constraints are lacking or contradictory (e.g. Camerota; Baggioni *et al.* 1981; Russo Ermolli 1999). In addition, the generally rich pollen assemblages from lacustrine sediments might reflect restricted vegetational and climatic conditions, which might be difficult to compare with the supraregional documentation of vegetation recorded in marine sediments (e.g. Comburieu-Nebout 1987). In the same Crotone Basin, Bertoldi (1977) and

Comburieu-Nebout (1987, 1995) reconstructed the vegetational and floral history within a robust chronological framework that covers the interval from 2.5 to 1.3 Ma, i.e. below that considered in our work. However, it can be observed that in our section the floral assemblage shows only subtle changes with respect to the Pliocene and Early Pleistocene. In fact, the major 'Tertiary' taxa (such as *Taxodium*, *Carya*, *Pterocarya*, *Liquidambar*, *Tsuga*, *Cedrus*) are still present, notwithstanding the likelihood that their contribution to the forest community composition became very low. Floristic data from the well-dated lacustrine succession of Sant'Arcangelo (southern Italy), which straddles the M-B boundary and is therefore coeval with the Valle di Manche section (Sabato *et al.* 2005), are apparently in agreement with our results (A. Bertini pers. comm.). Unfortunately, these data are at present not available to us.

We are not aware of marine pollen records from central Mediterranean marine sediments in the Middle Pleistocene interval. Only a single, well time-constrained lacustrine pollen record is available (i.e. the Vallo di Diano succession: Russo Ermolli 1994), which is located in the Campanian Apennines (NE of the Crotone area) and encompasses the interval from MIS 16 to MIS 13 (Russo Ermolli & Cheddadi 1997). Being slightly younger than the Valle di Manche section, this succession should reflect floral conditions younger than the time interval considered in our segment. The pollen checklist from Vallo di Diano is modern in overall character, being dominated by taxa present today in southern Italy. Nevertheless, some archaic taxa (e.g. *Tsuga*, *Cedrus*, *Taxodium* and Juglandaceae) still occur although with average values gradually declining with respect to the Valle di Manche record. It can be concluded that in the central Mediterranean area, the disappearance of 'Tertiary' taxa was a stepped, long-term phenomenon, rather than a dramatic collapse. Moreover, the EMPT apparently does not represent a time of dramatic breakthrough in the vegetation history of southern Italy. This conclusion strongly contrasts with what is observed in northern Italy, where the Taxodiaceae group underwent a massive decline at about the transition from the Late Pliocene to earliest Pleistocene (e.g. Lona & Bertoldi 1972; Mullenders *et al.* 1996).

MIS 19 and the Matuyama-Brunhes boundary

Although the M-B boundary is well recorded in numerous marine and lacustrine sediments, its exact age (within 10 ka) remains controversial. Since the work of Shackleton & Opdyke (1973), it has been established that the M-B boundary correlates to MIS 19, but its precise stratigraphic position within MIS

19 is not clear. Berger *et al.* (1995) placed it at the transition from MIS 20 to MIS 19, whereas Bassinot *et al.* (1994) and Channell & Kleiven (2000) placed it in the middle and upper parts of MIS 19, respectively. The planktonic oxygen isotope record from *G. ruber* at Valle di Manche (Figs 5 & 8) appears to display the substages of MIS 19 (19.1, 19.2, 19.3). These MIS 19 substages are, however, not generally seen in benthic (or planktonic) oxygen isotope records (Channell & Kleiven 2000, fig. 2). Interestingly, the other M–B boundary $\delta^{18}\text{O}$ record that shows the MIS 19 substages is also a planktonic record derived from *G. ruber* (Core MD900963 in Bassinot *et al.* 1994). Uncertainties in the exact position of the M–B boundary, both at Valle di Manche (Fig. 7) and in Core MD900963 (Bassinot *et al.* 1994), indicate that the M–B boundary cannot be precisely correlated to substages within the MIS 19.1–19.3 interval, but it does occur in the middle part of MIS 19.

Conclusions

We have studied oxygen isotope stratigraphy, pollen and planktonic foraminifera in the Valle di Manche section, located in the recently uplifted Crotona Basin in Calabria (southern Italy). The Matuyama–Brunhes boundary occurs within this section, which is characterized by a cyclothem organization caused, on the basis of physical stratigraphy and chronological constraints, by glacio-eustasy (Rio *et al.* 1996).

These new data presented lead to the following conclusions:

- (1) The glacio-eustatic origin of the two investigated cyclothem is confirmed.
- (2) Tectonics have strongly influenced the stratigraphic record of the San Mauro sub-basin (Massari *et al.* 2002), but the high-frequency and high-amplitude glacio-eustatic cycles that characterize the Pleistocene are preserved in the section, yielding a readable signal of climate-driven palaeoenvironmental changes.
- (3) Deposits from intervals of glacial maxima are preserved in the section, most probably because of the high tectonic subsidence; this is unusual for a shelf setting as demonstrated by Naish *et al.* (1998).
- (4) The interglacial deposits of MIS 21 are poorly preserved most probably because subsidence was not keeping pace with the small-amplitude precession-related eustatic oscillations that characterize this interglacial interval.
- (5) A more refined chronology has been established for the section. In particular, the pollen data suggest that the transgressive surface at the

base of cyclothem 8, that was not dated by Rio *et al.* (1996), most likely correlates to substage 18.3 (729 ka according to Bassinot *et al.* 1994). The derived chronology indicates an increase in subsidence at the transition from MIS 20 to MIS 19 that led to the deposition of expanded cyclothem 8 that is characterized by sediment accumulation rates in excess of 100 cm/ka.

- (6) The onset of the Brunhes Chron occurred in the middle part of MIS 19.
- (7) In the Crotona area, the glacial intervals of MIS 20 and 18 are characterized by alpine forest conditions, whereas a wooded steppe landscape became established at the beginning of the deglaciation from MIS 20 to MIS 19. These unexpected results are in stark contrast to previous views in which, in the central Mediterranean area, even in distant Pliocene and Early Pleistocene times, glacial intervals were thought to have been characterized by arid conditions. These findings emphasize the need for accurate correlation between the continental and marine climate in order to improve our understanding of land–sea interactions.

The authors are grateful to J.-P. Suc for carefully revising the manuscript and for providing many constructive comments. Suggestions by M. Follieri and M.J. Head helped significantly to improve the manuscript. This work was funded by MIUR (PRIN 1997) to D. Rio and (PRIN 1999–2001) to F. Massari.

References

- ACCORSI, C.A., BANDINI MAZZANTI, M. & FORLANI, L. 1978. Modello di schede palinologiche di Pini Italiani (*Pinus cembra* L., *Pinus pinea* L., *Pinus sylvestris* L. subsp. *syvestris* L. ecotipo emiliano). *Archivio Botanico e Biogeografico Italiano*, **54**, 65–101.
- ARMİ, L. & FARMER, D. 1985. The internal hydraulics of the Strait of Gibraltar and associated sills and narrows. *Oceanologica Acta*, **8**, 37–46.
- ASIOLI, A., TRINCARDI, F., LOWE, J.J., ARIZTEGUI, D., LANGONE, L. & OLDFIELD, F. 2001. Sub-millennial scale climatic oscillations in the Central Adriatic during the Late-glacial: paleoceanographic implications. *Quaternary Science Reviews*, **20**, 1201–1221.
- BAGGIONI, M., SUC, J.-P. & VERNET, J.L. 1981. Le Pliocène de Camerota (Italie méridionale): géomorphologie et paléoflores. *Geobios*, **14**, 229–237.
- BASSINOT, F.C., LABEYRIE, L.D., VINCENT, E., QUIDELLEUR, X., SHACKLETON, N.J. & LANCELOT, Y. 1994. The astronomical theory of climate and the age of the Brunhes–Matuyama magnetic reversal. *Earth and Planetary Science Letters*, **126**, 91–108.
- BERGER, W.H., YASUDA, M.K., BICKERT, T., WEFER, G. & TAKAYAMA, T. 1994. Quaternary time scale for the Ontong Java Plateau: Milankovitch template for Ocean Drilling Program Site 806. *Geology*, **22**, 463–467.

- BERGER, W.H., BICKERT, T., WEFER, G. & YASUDA, M.K. 1995. Brunhes–Matuyama boundary: 790 k.y. date consistent with ODP Leg 130 oxygen isotope records based on fit to Milankovitch template. *Geophysical Research Letters*, **22**, 1525–1528.
- BERTINI, A. 2001. Pliocene climatic cycles and altitudinal forest development from 2.7 Ma in the Northern Apennines (Italy): evidence from the pollen record of the Stirone section (~5.1 to ~2.2 Ma). *Geobios*, **34**, 253–265.
- BERTINI, A. 2003. Early to middle Pleistocene changes in the Italian flora and vegetation in the light of a chronostratigraphic framework. *Il Quaternario*, **16**, 19–36.
- BERTOLDI, R. 1977. Studio palinologico della serie di Le Castella (Calabria). *Rendiconti dell'Accademia Nazionale dei Lincei*, **62**, 547–555.
- BIJMA, J., FABER, W.W. Jr. & HEMLEBEN, C. 1990. Temperature and salinity limits for growth and survival of some planktonic foraminifers in laboratory cultures. *Journal of Foraminiferal Research*, **20**, 95–116.
- BRYDEN, H.L. & KINDER, T.H. 1991. *Recent Progress in Strait Dynamics. Review of Geophysics*, Supplement, US National Report to International Union of Geodesy and Geophysics 1987–1990, 617–631.
- CAPOTONDI, L., BORSETTI, A.M. & MORIGI, C. 1999. Foraminiferal ecozones, a high resolution proxy for the late Quaternary biochronology in the central Mediterranean Sea. *Marine Geology*, **153**, 253–274.
- CHANNELL, J.E.T. & KLEIVEN, H. 2000. Geomagnetic palaeointensities and astrochronological ages for the Matuyama–Brunhes boundary and the Jaramillo Subchron: Palaeomagnetic and oxygen isotope records from ODP Site 983. *Philosophical Transactions of the Royal Society*, **358**, 1027–1047.
- Comburieu-Nebout, N. 1987. *Les premiers cycles glaciaire–interglaciaire en région méditerranéenne d'après l'analyse palinologique de la série plio-pléistocène de Crotona (Italie méridionale)*. Doctoral thesis, University of Montpellier.
- FENAROLI, L. 1971. Note illustrative della carta della vegetazione reale d'Italia. Pubblicazioni del Ministero dell'Agricoltura e delle Foreste, Roma.
- FOLLIERI, M., MAGRI, D. & SADORI, L. 1988. 250,000-year pollen record from Valle di Castiglione (Roma). *Pollen et Spores*, **30**, 329–356.
- FROSINI, P. 1961. *La Carta della precipitazione media annua in Italia per il trentennio 1921–1950*. Monografie del Servizio Idrografico Nazionale, **24**.
- GELLINI, R. & GROSSONI, P. 1997. *Botanica forestale. Vol. II: Angiosperme*. CEDAM, Padova.
- HAYES, A., ROHLING, E.J., DE RIJK, S., KROON, D. & ZACHARIASSE, W.J. 1999. Mediterranean planktonic foraminiferal faunas during the last glacial cycle. *Marine Geology*, **153**, 239–252.
- HEMLEBEN, C., SPINDLER, M. & ANDERSON, O.R. 1989. *Modern Planktonic Foraminifera*. Springer-Verlag, New York.
- JORISSEN, F.J., ASIOLI, A. ET AL. 1993. Late Quaternary central Mediterranean biochronology. *Marine Micropaleontology*, **21**, 169–189.
- KUKLA, G. & CILEK, V. 1996. Plio-Pleistocene megacycles: record of climate and tectonics. *Palaeogeography, Palaeoclimatology, Palaeoecology*, **120**, 171–194.
- LANGEREIS, C.G., DEKKERS, M.J., DE LANGE, G.J., PATERNE, M. & VAN SANTVOORT, P.J.M. 1997. Magnetostratigraphy and astronomical calibration of the last 1.1 Myr from an eastern Mediterranean piston core and dating of short events in the Brunhes. *International Journal of Geophysics*, **129**, 75–94.
- LONA, F. & BERTOLDI, R. 1972. La storia del Plio-Pleistocene italiano in alcune sequenze lacustri e marine. *Memorie dell'Accademia Nazionale dei Lincei*, **8**, 1–47.
- MASSARI, F., SGAVETTI, M., RIO, D., D'ALESSANDRO, A. & PROSSER, G. 1999. Sedimentary record of falling stages of Pleistocene glacio-eustatic cycles in shelf setting (Crotona Basin, south Italy). *Sedimentary Geology*, **127**, 85–110.
- MASSARI, F., RIO, D. ET AL. 2002. Interplay between tectonics and glacio-eustasy: Pleistocene succession of the Crotona Basin, Calabria (Southern Italy). *Geological Society of America Bulletin*, **114**, 1183–1209.
- MUDELSEE, M. & SCHULZ, M. 1997. The Mid-Pleistocene climate transition: onset of 100 ka cycle lags ice volume build-up by 280 ka. *Earth and Planetary Science Letters*, **151**, 117–123.
- MULLENDERS, W., FAVERO, V., COREMANS, M. & DIRICKX, M. 1996. Analyses polliniques de sondages a Venise (VE-I, VE-I bis, VE-II). *Aardkundige Mededelingen*, **7**, 87–117.
- NAISH, T.R., ABBOTT, S.T. ET AL. 1998. Astronomical calibration of a southern Hemisphere Plio-Pleistocene reference section, Wanganui Basin, New Zealand. *Quaternary Science Reviews*, **17**, 695–710.
- NOIRFALISE, A., DAHL, E. ET AL. 1987. *Carte de la végétation naturelle des Etats membres des Communautés européennes et du Conseil de l'Europe*. Office des publications des Communautés européennes.
- PIGNATTI, S. 1979. I piani di vegetazione in Italia. *Giornale Botanico Italiano*, **113**, 411–428.
- PILLANS, B. 2003. Subdividing the Pleistocene using the Matuyama–Brunhes Boundary (MBB): an Australian perspective. *Quaternary Science Reviews*, **22**, 1569–1577.
- POLI, M.S. 1995. *Foraminiferi bentonici e ciclicità nel Pleistocene di piattaforma del Bacino di Crotona*. Doctoral thesis, University of Padova.
- PRELL, W.L. 1982. Oxygen and carbon isotopic stratigraphy for the Quaternary of hole 502B: Evidence for two modes of isotopic variability. *Initial Reports of the Deep Sea Drilling Project*, **68**, 455–464.
- PROKOPENKO, A.A., WILLIAMS, D.F., KUZMIN, M.I., KARABANOV, E.B., KHURSEVICH, G.K. & PECK, J. 2002. Muted climate variations in continental Siberia during the mid-Pleistocene epoch. *Nature*, **418**, 65–68.
- PUJOL, C. & VERGNAUD-GRAZZINI, C. 1995. Distribution patterns of live planktonic foraminifera as related to regional hydrography and productive systems of the Mediterranean Sea. *Marine Micropaleontology*, **25**, 187–217.
- QUÉZEL, P., BARBERO, M., BONIN, G. & LOISEL, R. 1980. Essai de corrélations phytosociologique et bioclimatiques entre quelques structure actuelles et passées de la végétation méditerranéenne. *Naturalia Monspeliensia*, extraseries, 89–100.

- RAYMO, M.E., OPPO, D.W. & CURRY, W. 1997. The mid-Pleistocene climate transition: A deep sea carbon isotopic perspective. *Paleoceanography*, **12**, 546–559.
- RICHMOND, G.M. 1996. The INQUA-approved provisional Lower-Middle Pleistocene boundary. In: TURNER, C. (ed.) *The Early–Middle Pleistocene in Europe*. Balkema, Rotterdam, 319–326.
- RIO, D., CHANNELL, J.E.T., MASSARI, F., POLI, M.S., SGAVETTI, M., D'ALESSANDRO, A. & PROSSER, G. 1996. Reading Pleistocene eustasy in a tectonically active siliciclastic shelf setting (Crotona peninsula, Southern Italy). *Geology*, **24**, 743–746.
- RODA, C. 1964. Distribuzione e facies dei sedimenti Neogenici del Bacino Crotonese. *Geologica Romana*, **3**, 319–366.
- ROSSIGNOL-STRICK, M. & PATERNE, M. 1999. A synthetic pollen record of the eastern Mediterranean sapropels of the last 1 Ma: implications for the time-scale and formation of sapropels. *Marine Geology*, **153**, 221–237.
- RUDDIMAN, W.F., RAYMO, M.E., MARTINSON, D.G., CLEMENT, B.M. & BACKMAN, J. 1989. Pleistocene Evolution: Northern Hemisphere Ice Sheets and North Atlantic Ocean. *Paleoceanography*, **4**, 353–412.
- RUSSO ERMOLLI, E. 1994. Analyse pollinique de la succession lacustre pléistocène du Vallo di Diano (Campanie, Italie). *Annales de la Société Géologique du Belgique*, **117**, 333–354.
- RUSSO ERMOLLI, E. 1999. Vegetation dynamics and climate changes at Camerota (Campania, Italy) at the Pliocene–Pleistocene boundary. *Il Quaternario*, **12**, 207–214.
- RUSSO ERMOLLI, E. & CHEDDADI, R. 1997. Climatic reconstruction during the Middle Pleistocene: a pollen record from Vallo di Diano (southern Italy). *Geobios*, **30**, 735–744.
- SABATO, L., BERTINI, A., MASINI, F., ALBIANELLI, A., NAPOLEONE, G. & PIERI, P. 2005. The lower and middle Pleistocene geological record of the San Lorenzo lacustrine sequence in Sant'Arcangelo Basin (Southern Apennines, Italy). *Quaternary International*, **131**, 59–69.
- SANVOISIN, R., D'ONOFRO, S., LUCCHI, R., VIOLANTI, D. & CASTRADORI, D. 1993. 1 Ma palaeoclimatic record from the Eastern Mediterranean–Marflux project: first results of a micropaleontological and sedimentological investigation of a long piston core from the Calabrian Ridge. *Il Quaternario*, **6**, 169–188.
- SBAFFI, L., WEZEL, F.C. & SHACKLETON, N.J. 1998. Paleoclimatologia dell'ultima deglaciazione nel Bacino di Cefalù – Mar Tirreno meridionale. *Rendiconti dell'Accademia Nazionale dei Lincei*, **9**, 177–200.
- SBAFFI, L., WEZEL, F.C., KALLEL, N., PATERNE, M., CACHO, I., ZIVERI, P. & SHACKLETON, N.J. 2001. Response of the pelagic environment to palaeoclimatic changes in the Central Mediterranean Sea during the Late Quaternary. *Marine Geology*, **178**, 39–62.
- SHACKLETON, N.J. & OPDYKE, N.D. 1973. Oxygen-isotope and paleomagnetic stratigraphy of Pacific core V28–239, late Pliocene to latest Pleistocene. *Memoirs of the Geological Society of America*, **145**, 449–464.
- SHACKLETON, N.J., BERGER, A. & PELTIER, W.R. 1990. An alternative astronomical calibration of the lower Pleistocene timescale based on ODP Site 677. *Transactions of the Royal Society of Edinburgh, Earth Sciences*, **81**, 251–261.
- STOCKMARR, J. 1971. Tablets with spores used in absolute pollen analysis. *Pollen et Spores*, **13**, 615–621.
- SUC, J. -P. 1976. Quelques taxons-guides dans l'étude paléoclimatique du Pliocène et du Pléistocène inférieur du Languedoc (France). *Revue de Micropaléontologie*, **18**, 246–255.
- SUC, J. -P., CLAUZON, G. ET AL. 1992. Neogene and lower Pleistocene in Southern France and Northeastern Spain. Mediterranean environments and climate. *Cahiers de Micropaléontologie*, **7**, 165–186.
- THUNELL, R.C. & WILLIAMS, D.F. 1989. Glacial–Holocene salinity changes in the Mediterranean Sea: hydrographic and depositional effects. *Nature*, **338**, 493–496.
- TZEDAKIS, P.C., ANDRIEU, V., ET AL. 1997. Comparison of terrestrial and marine records of changing climate of the last 500,000 years. *Earth and Planetary Science Letters*, **150**, 171–176.
- VAN CAMPO-DUPLAN, M. 1950. Recherches sur la phylogénie des Abetineses d'après leurs grains de pollen. *Travaux du Laboratoire Forestier de Toulouse*, **2**, 1–178.
- VAN DIJK, J.P. 1991. Basin dynamics and sequence stratigraphy in the Calabrian Arc (Central Mediterranean); records and pathways of the Crotona Basin. *Geologie en Mijnbouw*, **70**, 187–201.
- VERGNAUD-GRAZZINI, C., RYAN, W.B.F. & CITA, M.B. 1977. Stable isotopic fractionation, climate change and episodic stagnation in the eastern Mediterranean during the late Quaternary. *Marine Micropaleontology*, **2**, 353–370.
- VERGNAUD-GRAZZINI, C., GLACON, G., PIERRE, C., PUJOL, C. & URRUTIAGUER, M.J. 1986. Foraminifères planctoniques de Méditerranée en fin d'été. Relations avec les structures hydrologiques. *Memorie della Società geologica Italiana*, **36**, 175–188.
- WÆLBROEK, C., LABEYRIE, L. ET AL. 2002. Sea level and deep water temperature changes derived from benthic foraminifera isotopic records. *Quaternary Science Review*, **21**, 295–305.
- WALTER, H. 1974. Die Vegetation Osteuropas, Nord-und Zentralaziens. Fischer Verlag, Stuttgart.
- WILLIAMS, D.F., KUZMIN, M.I., PROKOPENKO, A.A., KARABANOV, E.B., KHURSEVICK, G.K. & BEZRUKOVA, E.V. 2001. The Lake Baikal drilling project in the context of a global lake drilling initiative. *Quaternary International*, **80–81**, 3–18.